Generalized Polarizabilities of the proton

Status and new results

Nikos Sparveris

Temple University

9th International Conference of Quarks & Nuclear Physics

QNP 2022

Supported by the US DOE / NP award DE-SC0016577

Outline

Brief Introduction to the GPs

Overview – current status

Recent results

Prospects

Proton Polarizablities

Fundamental structure constants (such as mass, size, shape, …)

Response of internal structure & dynamics to external EM field

Sensitive to the full excitation spectrum of the nucleon

Accessed experimentally through Compton Scattering processes

RCS: static polarizabilities
→ net effect on the nucleon

PDG

150 Baryon Summary Table

N BARYONS
$(S = 0, I = 1/2)$
$p, N^+ = uud; \quad n, N^0 = udd$

p $\quad I(J^P) = \frac{1}{2}(\frac{1}{2}^+)$

Mass $m = 1.00727646681 \pm 0.00000000009$ u
Mass $m = 938.272046 \pm 0.000021$ MeV [a]
$|m_p - m_{\overline{p}}|/m_p < 7 \times 10^{-10}$, CL = 90% [b]
$|\frac{q_{\overline{p}}}{m_{\overline{p}}}|/(\frac{q_p}{m_p}) = 0.99999999991 \pm 0.00000000009$
$|q_p + q_{\overline{p}}|/e < 7 \times 10^{-10}$, CL = 90% [b]
$|q_p + q_e|/e < 1 \times 10^{-21}$ [c]
Magnetic moment $\mu = 2.792847356 \pm 0.000000023\ \mu_N$
$(\mu_p + \mu_{\overline{p}}) / \mu_p = (0 \pm 5) \times 10^{-6}$
Electric dipole moment $d < 0.54 \times 10^{-23}$ e cm
Electric polarizability $\alpha = (11.2 \pm 0.4) \times 10^{-4}$ fm^3
Magnetic polarizability $\beta = (2.5 \pm 0.4) \times 10^{-4}$ fm^3 (S = 1.2)
Charge radius, μp Lamb shift $= 0.84087 \pm 0.00039$ fm [d]
Charge radius, $e p$ CODATA value $= 0.8775 \pm 0.0051$ fm [d]
Magnetic radius $= 0.777 \pm 0.016$ fm
Mean life $\tau > 2.1 \times 10^{29}$ years, CL = 90% [e] ($p \rightarrow$ invisible mode)
Mean life $\tau > 10^{31}$ to 10^{33} years [e] (mode dependent)

Virtual Compton Scattering:

Virtuality of photon gives access to the GPs : $\alpha_E(Q^2)$ & $\beta_M(Q^2)$ (+ 4 spin GPs)

➔ mapping out the spatial distribution of the polarization densities

Fourier transform of densities of electric charges and magnetization of a nucleon deformed by an applied EM field

Scalar Polarizablities

Response of internal structure to an applied EM field

Interaction of the EM field with the internal structure of the nucleon

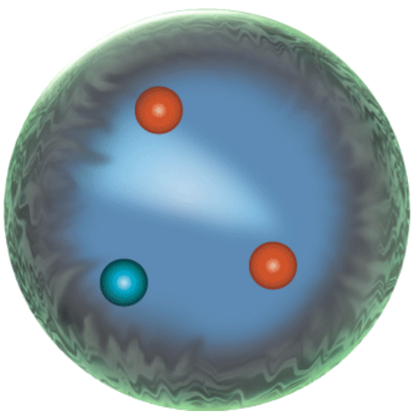

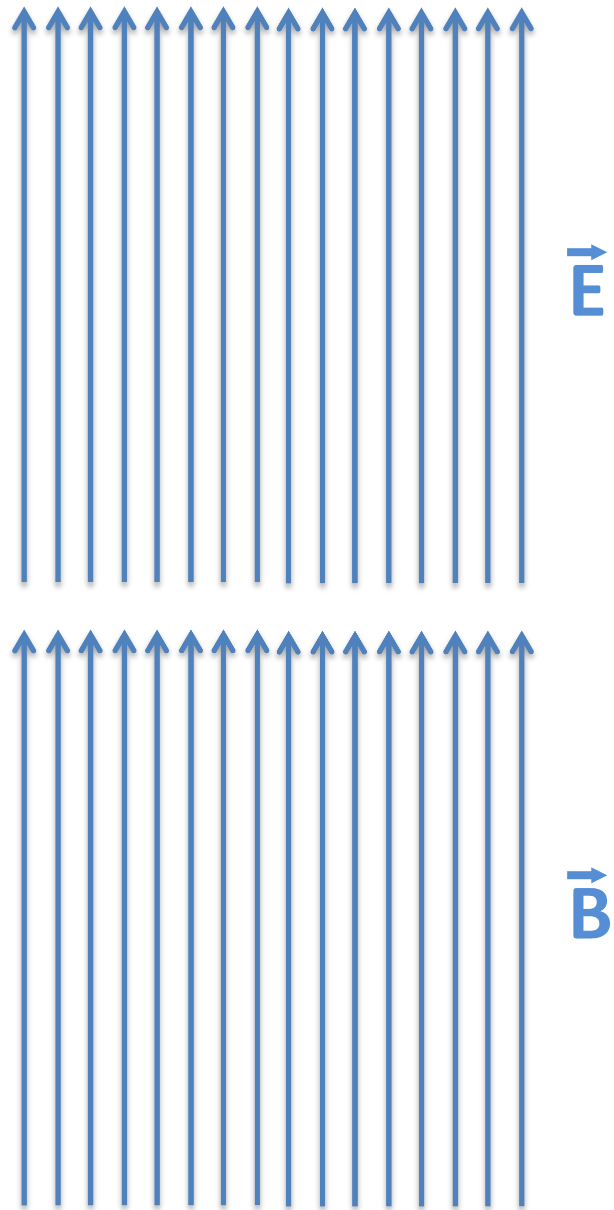

Scalar Polarizablities

Response of internal structure to an applied EM field

Interaction of the EM field with the internal structure of the nucleon

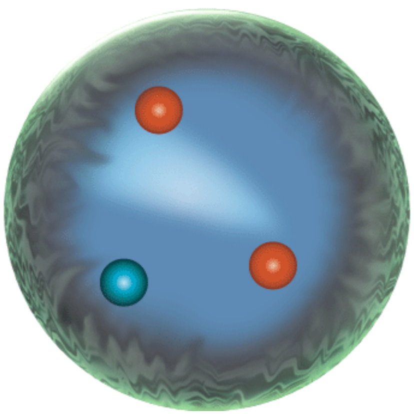

Compton scattering amplitude expanded in the photon energy:

2^{nd} order contribution

$$H_{\text{eff}}^{(2)} = -4\pi \left(\tfrac{1}{2}\,\alpha_{E1}\,\boldsymbol{E}^2 + \tfrac{1}{2}\,\beta_{M1}\,\boldsymbol{H}^2\right)$$

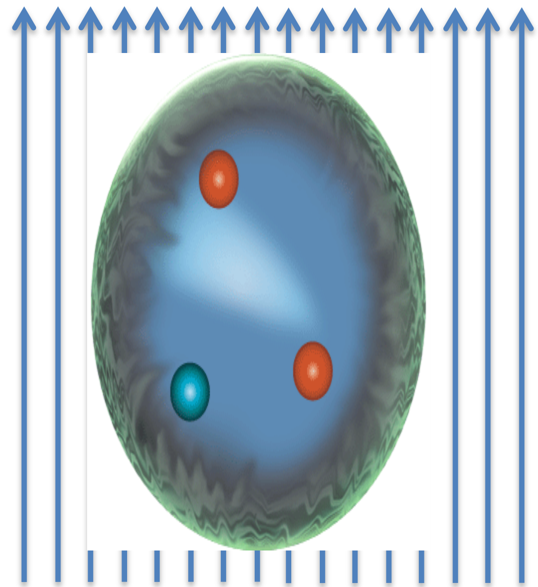

$\vec{E}$

"stretchability"

$\vec{d}_{E\ \text{induced}} \sim \alpha\,\vec{E}$

External field deforms the charge distribution

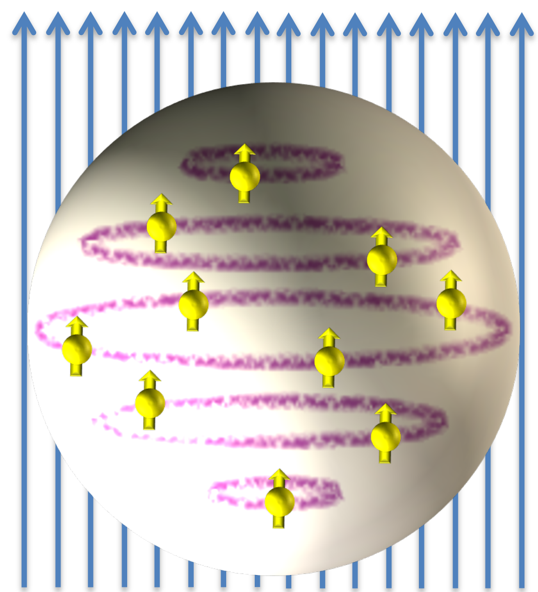

$\vec{B}$

"alignability"

$\vec{d}_{M\ \text{induced}} \sim \beta\,\vec{B}$

$\beta_{para} > 0$

$\beta_{diam} < 0$

Paramagnetic: proton spin aligns with the external magnetic field

Diamagnetic: π-cloud induction produces field counter to the external one

Virtual Compton Scattering

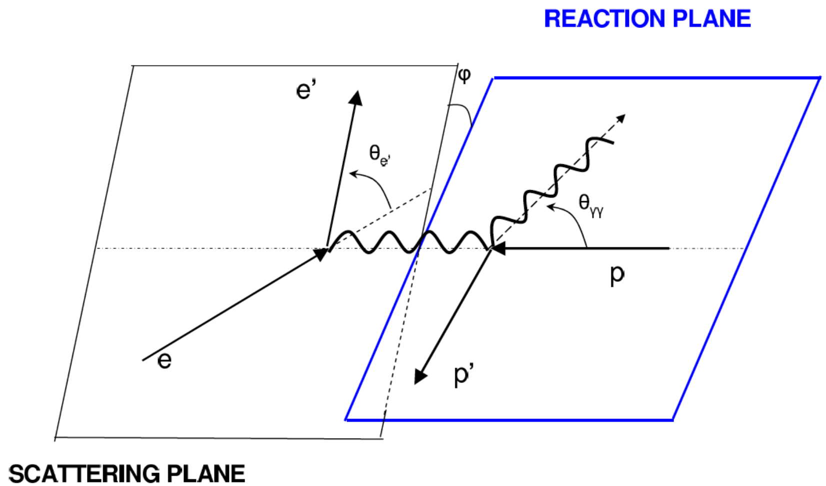

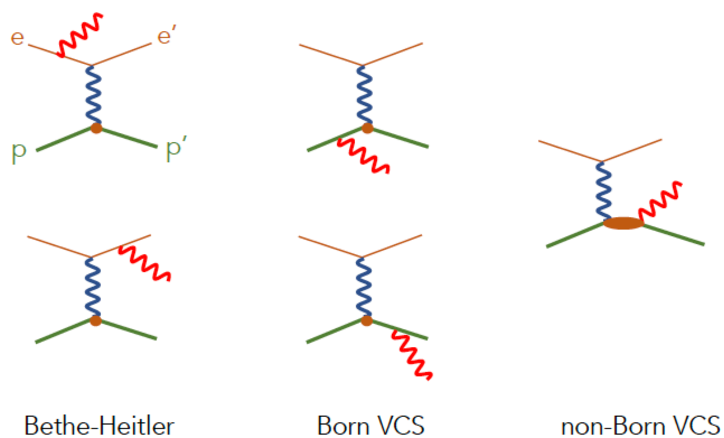

Elastic FFs

GPs

Virtual Compton Scattering

DR

valid below & above
Pion threshold

Dispersive integrals
for Non Born amplitudes

Spin GPs are fixed

Scalar GPs have
an unconstrained part

Fit to the experimental
cross sections at each Q^2

LEX

valid only below
Pion threshold

Structure functions

$$d^5\sigma = d^5\sigma^{BH+Born} + q'_{cm} \cdot \phi \cdot \Psi_0 + \mathcal{O}(q'^2_{cm})$$

$$\Psi_0 = v_1 \cdot (P_{LL} - \frac{1}{\epsilon} P_{TT}) + v_2 \cdot P_{LT}$$

Subtract the spin part

$$P_{TT} = [P_{TT\ spin}]$$

$$P_{LT} = -\frac{2M}{\alpha_{em}} \sqrt{\frac{q^2_{cm}}{Q^2}} \cdot G^p_E(Q^2) \cdot \beta_M(Q^2) + [P_{LT\ spin}]$$

utilize DR

scalar GPs α_E and β_M

Virtual Compton Scattering

Phys. Rev C 86, 015210 (2012)

Phys. Rev Lett. 93, 122001 (2004)

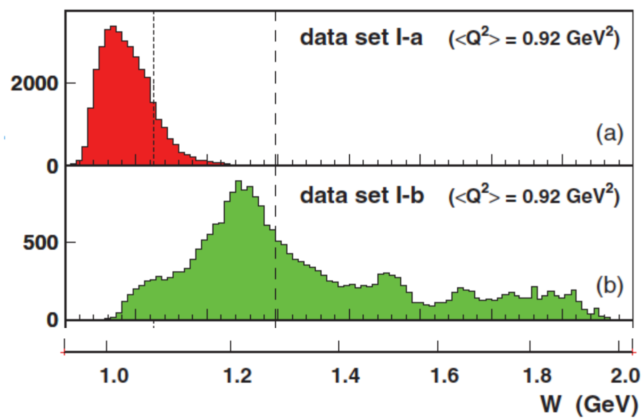

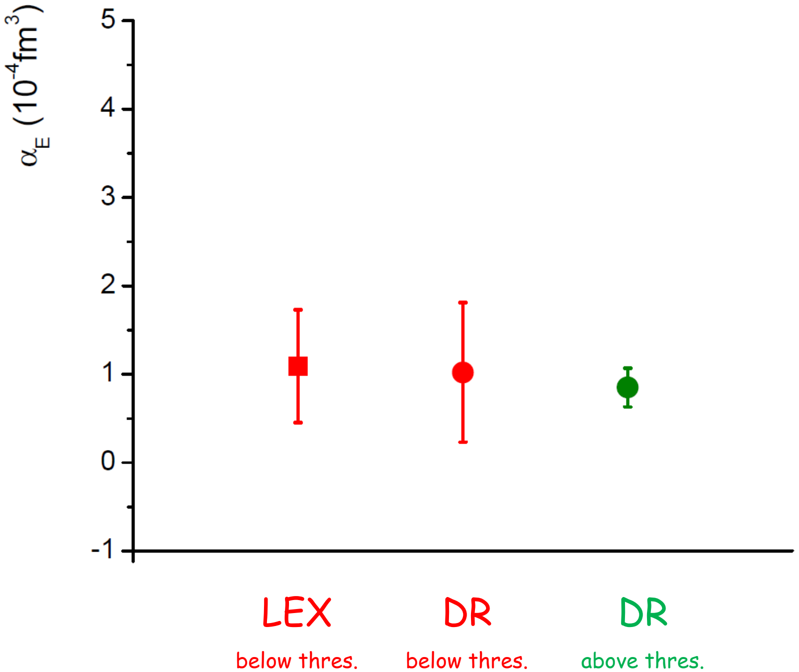

Sensitivity to the GPs grows as we measure above pion threshold

Early Experiments

MIT-Bates @ Q^2=0.06 GeV^2

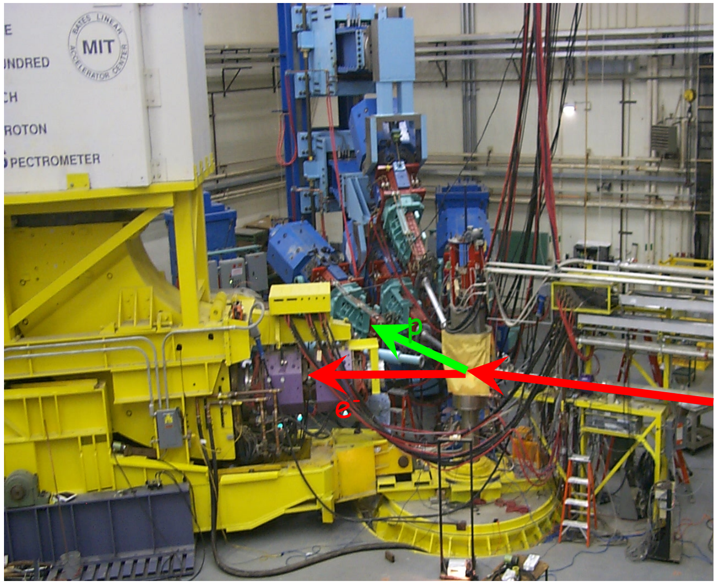

MAMI-A1 @ Q^2=0.33 GeV^2

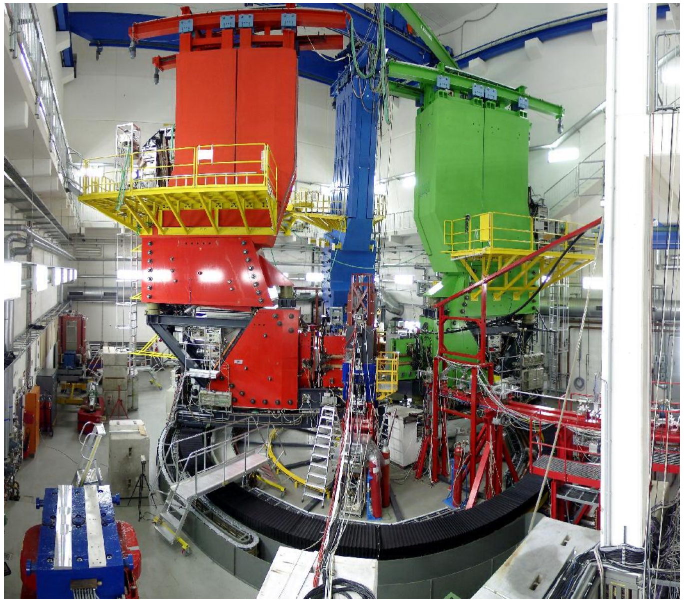

Jlab-Hall A @ Q^2=0.9 & 1.8 GeV^2

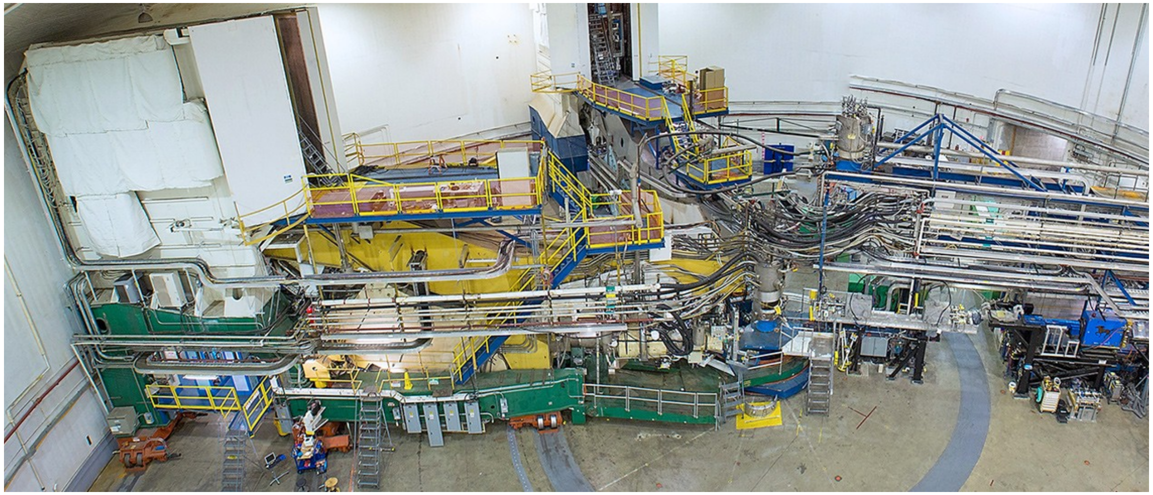

Early Experiments

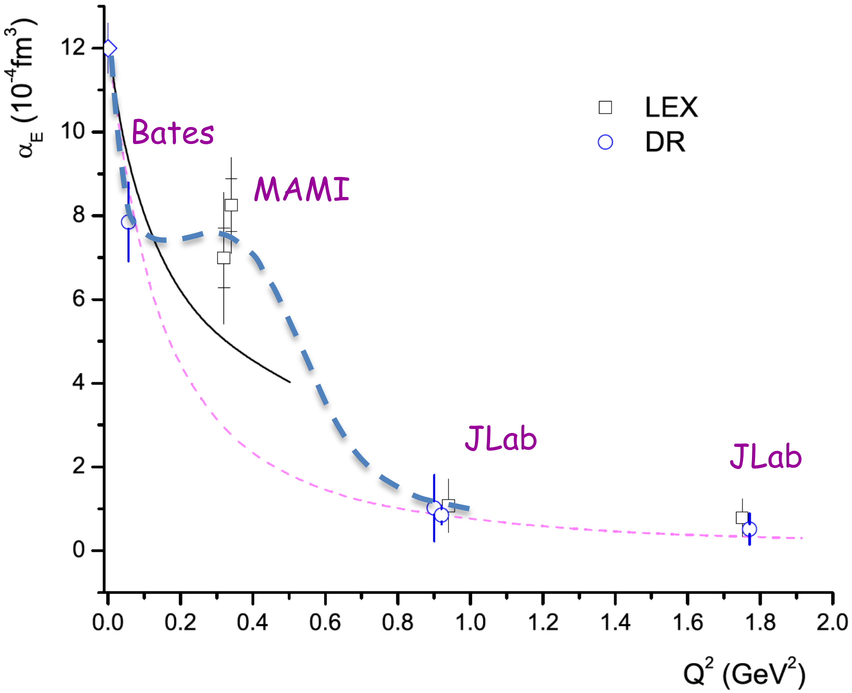

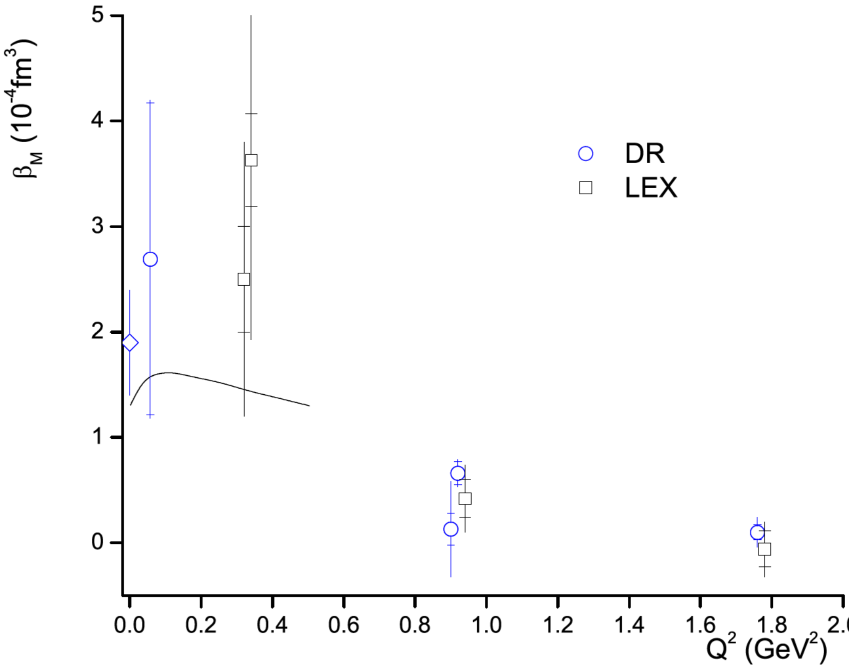

$\alpha_E \approx 10^{-3} V_N$ (stiffness / relativistic character)

Data suggest non-trivial Q^2 evolution of α_E

Current theoretical calculations not able to describe the enhancement at low Q^2

$Q^2 = 0.33\ (\mathrm{GeV}/c)^2$ measured twice at MAMI:

- Phys. Rev. Lett 85, 708 (2000)
- Eur. Phys. J. A37, 1-8 (2008)

β_M small ←→ cancellation of competing mechanisms

Large uncertainties

Higher precision measurements needed

→ Quantify the balance between diamagnetism and paramagnetism

Theory

T.R. Hemmert et al — Phys. Rev. D 62, 014013 (2000)

B. Pasquini et al — Phys. Rev. C 63, 025205 (2001)

A. Yu. Korchin and O. Scholten — Phys. Rev. C 58, 1098 (1998)

A. Metz and D. Drechsel — Z. Phys. A 356, 351 (1996)

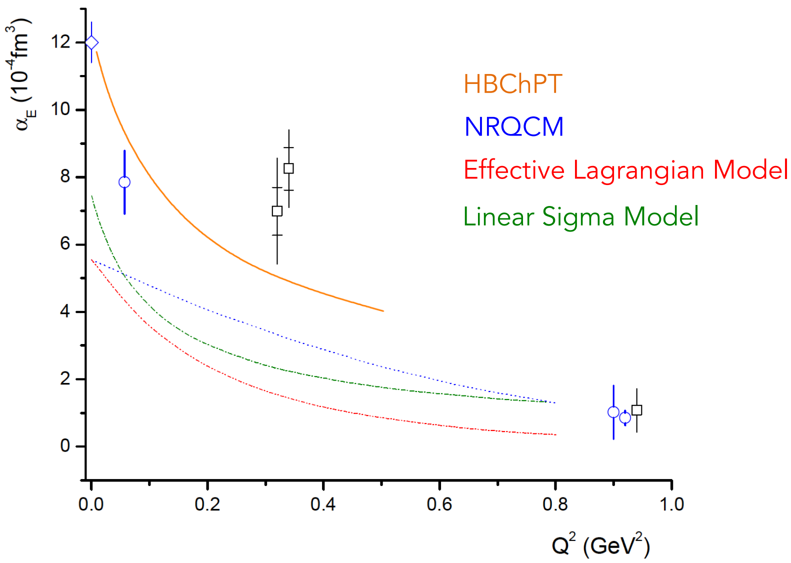

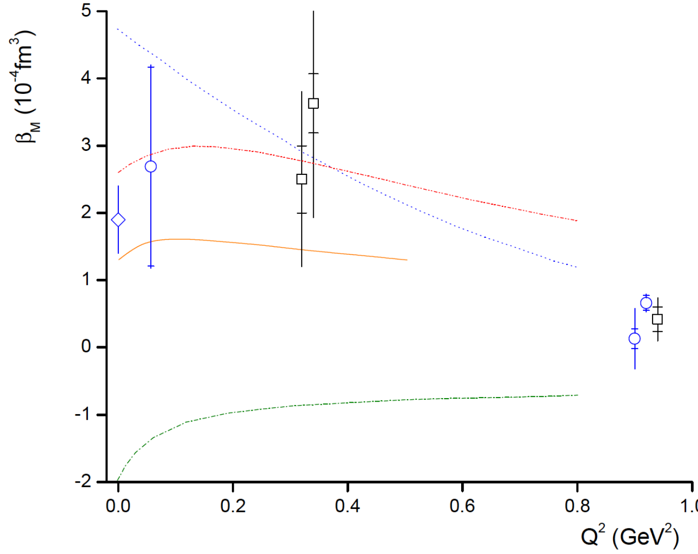

Theoretical calculations predict a smooth fall off for $\boldsymbol{\alpha}_E$

Can not account for the non-trivial structure of $\boldsymbol{\alpha}_E$ suggested by the data

Lattice QCD: No calculations for the GPs yet

Recent Measurements: MAMI

MAMI	A1/1-09 (vcsq2)	below threshold
MAMI	A1/3-12 (vcsdelta)	above threshold

Both experiments utilized the A1 setup at MAMI

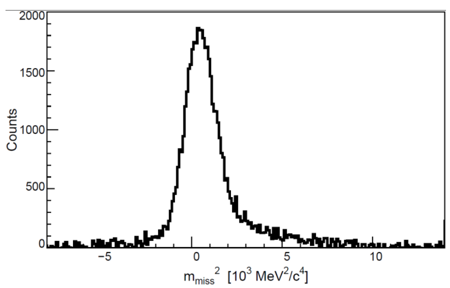

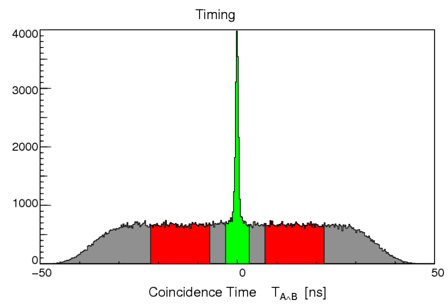

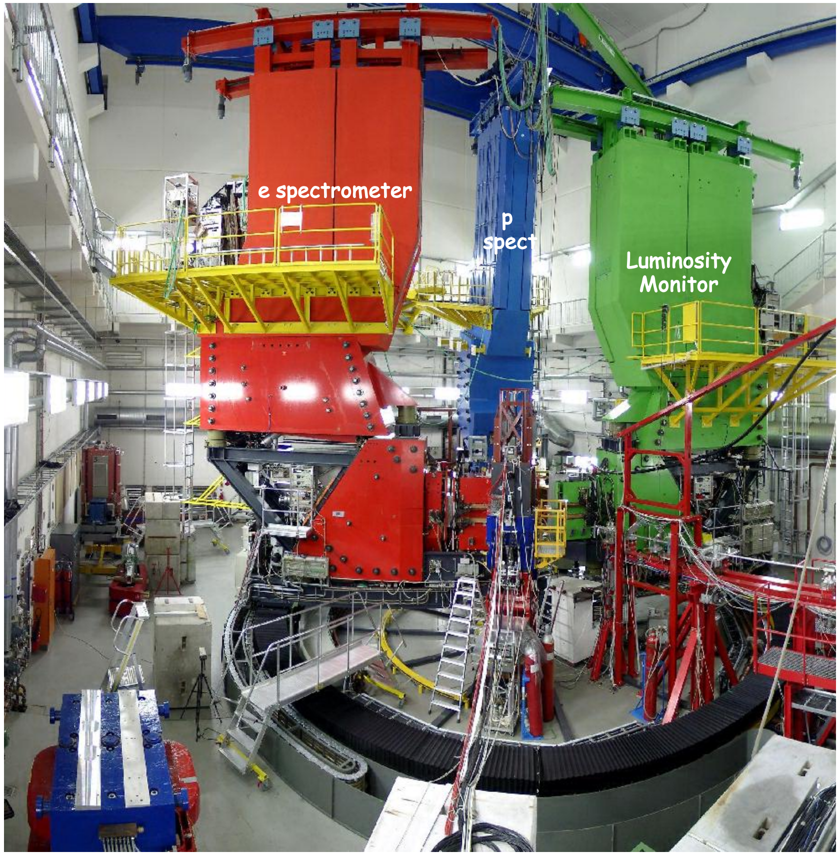

A1/1-09 @ MAMI

For LEX the higher order terms have to be negligible

$$d^5\sigma \;=\; d^5\sigma^{BH+Born} \;+\; q'_{cm}\cdot\phi\cdot\Psi_0 \;+\; \mathcal{O}(q'^2_{cm})$$

A phase space masking has to be applied to keep these terms smaller than the 2%-3% level

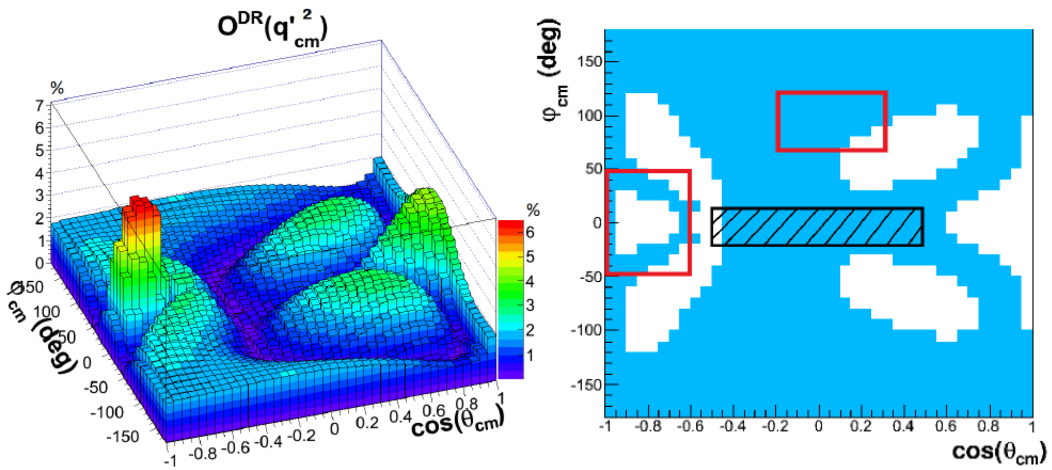

Figure 3.13: (Left) behavior of $\mathcal{O}^{DR}({q'_{cm}}^2)$ in the $(cos(\theta_{cm}),\varphi_{cm})$-plane at $q'_{cm} = 87.5\ MeV/c$ and (right) two-dimensional representation of the angular region where $\mathcal{O}^{DR}({q'_{cm}}^2) < 2\%$ (blue), the red squares correspond to the two areas of interest to perform the GP extraction.

Figure from PhD thesis of L. Correa, Mainz / Cl. Ferrand

Blue bins = where the higher-order estimator is < 3%
(LEX truncation « valid »)

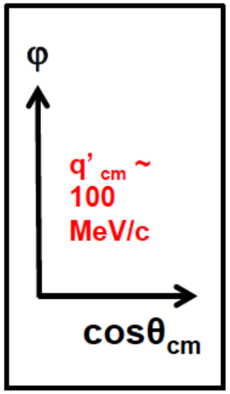

VCS expt :	Bates	MAMI	MAMI	MAMI	MAMI	JLab
Q2 (GeV2) =	0.06	0.10	0.20	0.33	0.45	0.92

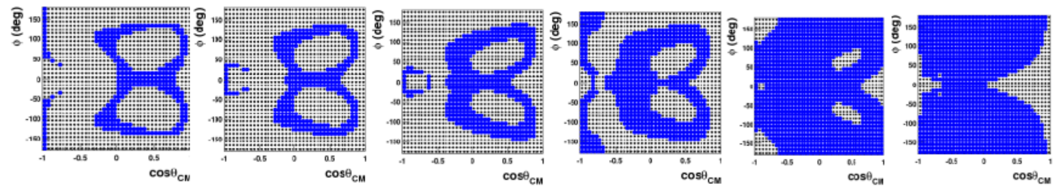

New « vcsq2 » data:

- OOP kinematics (to access the blue region)

-LEX Fit done with bin selection at Q^2 = 0.1 and 0.2 GeV^2.

- was found not necessary at Q^2 = 0.45 GeV^2.

In-plane

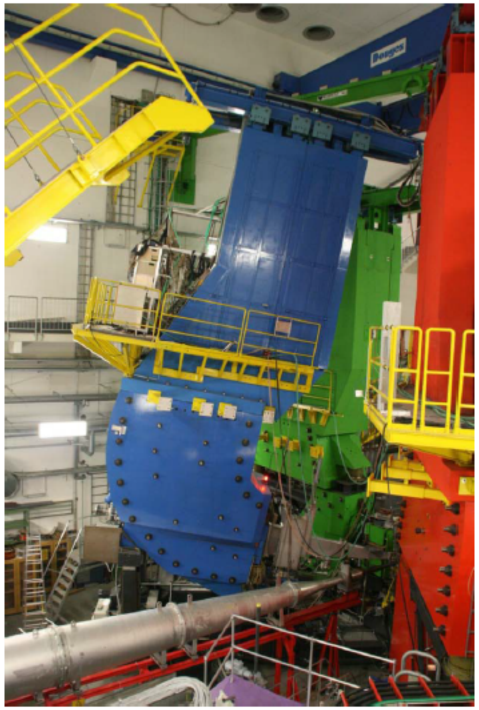

8.5 deg OOP

(material from H. Fonvieille)

A1/1-09 @ MAMI

~ 1.0 GeV beam

Q^2 = 0.1 $(GeV/c)^2$, 0.2 $(GeV/c)^2$, and 0.45 $(GeV/c)^2$

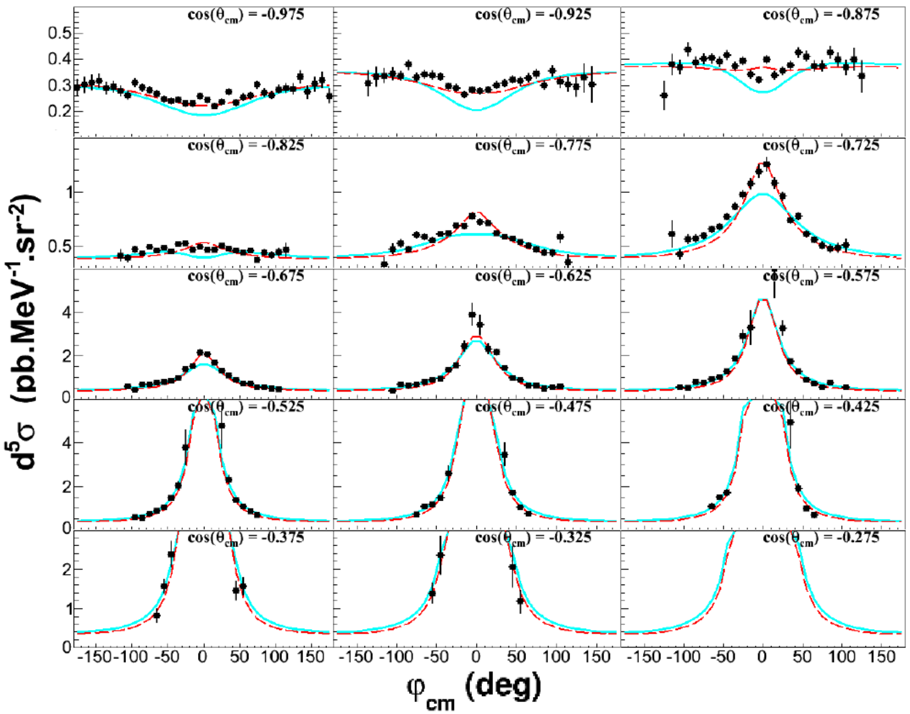

Figure 5.8: Setting INP: measured $ep \to ep\gamma$ cross section at fixed q'_{cm} = 112.5 MeV/c with respect to φ_{cm} for all the $cos(\theta_{cm})$-bins. The curves follow the convention of figure 5.6.

Figure from PhD thesis of L. Correa, Mainz / Cl. Ferrand

BH+B ---

Polarizability effect ---

GP effect typically 5% - 15% of the cross section

Polarizability fits:

DR fit:
DR calculation includes full dependency in q'_{cm}

LEX fit:
truncated in q'cm. Suppress contribution from higher order terms

A1/1-09 Results

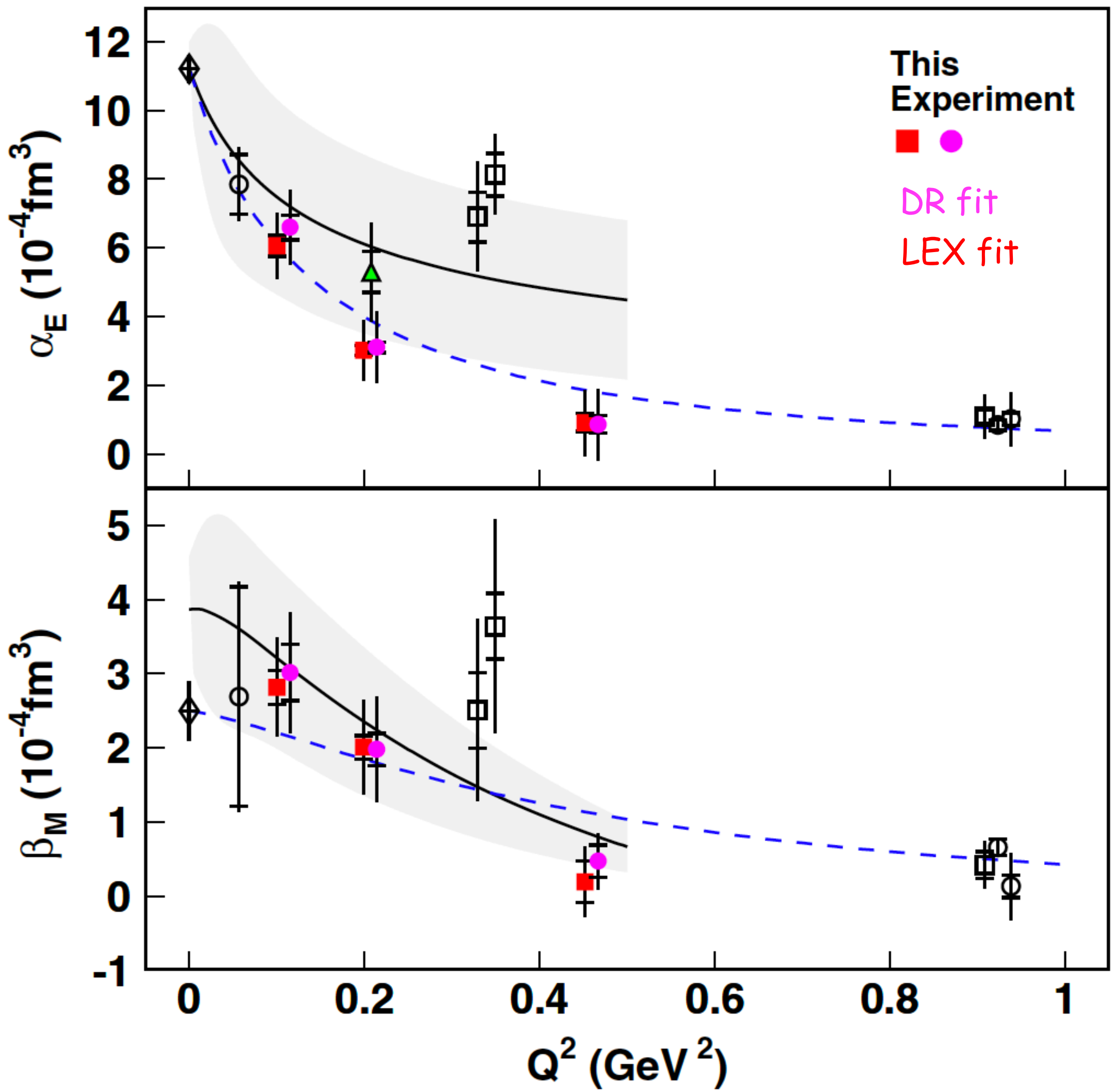

A1/3-12 @ MAMI

Goal 2-fold: 1) Measurement of the electric GP α_E

2) First measurement of N->Δ transition form factors through the γ channel

1.1 GeV beam, 5cm LH_2, spectrometers A & B in coinc.

Measurement at Q^2 = 0.2 $(GeV/c)^2$

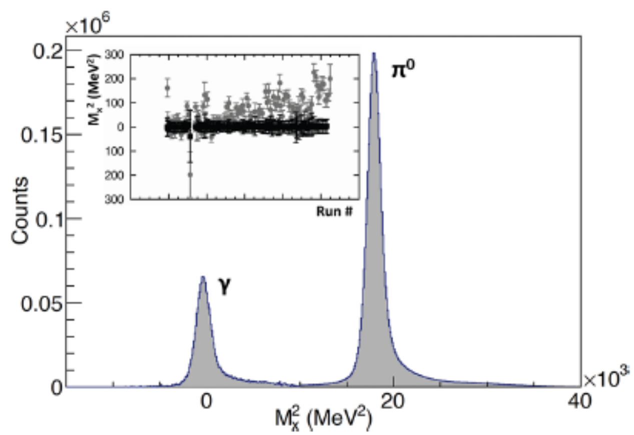

Fig. 1. The missing mass spectrum. The two peaks corresponding to the photon and to the π^0 are very well separated. The photon peak has been multiplied by a factor of 10 so that it can be clearly seen in the figure. The inserted panel shows the center of the photon missing mass peak before (gray circle) and after (black box) the momentum calibration as a function of the different run numbers.

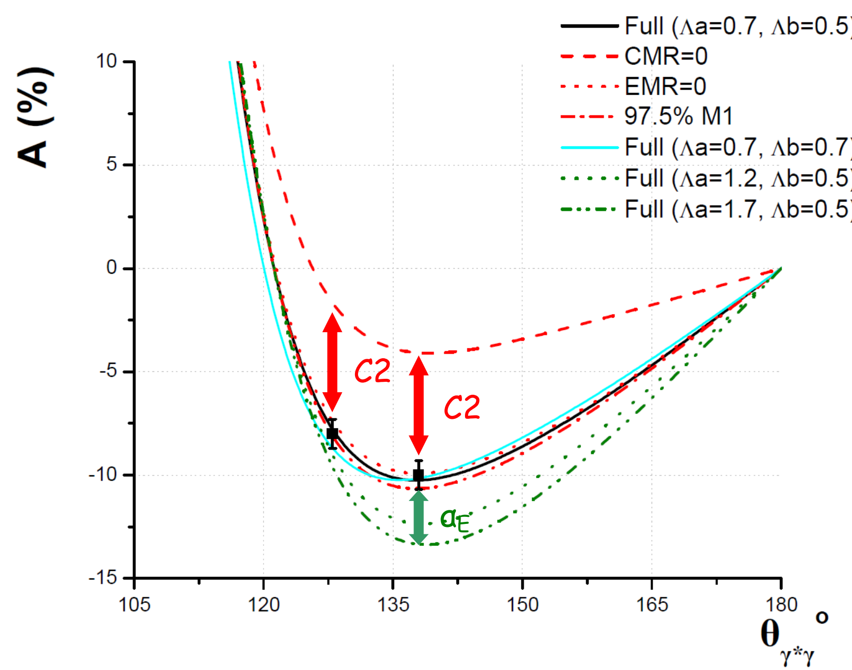

A1/3-12 Results

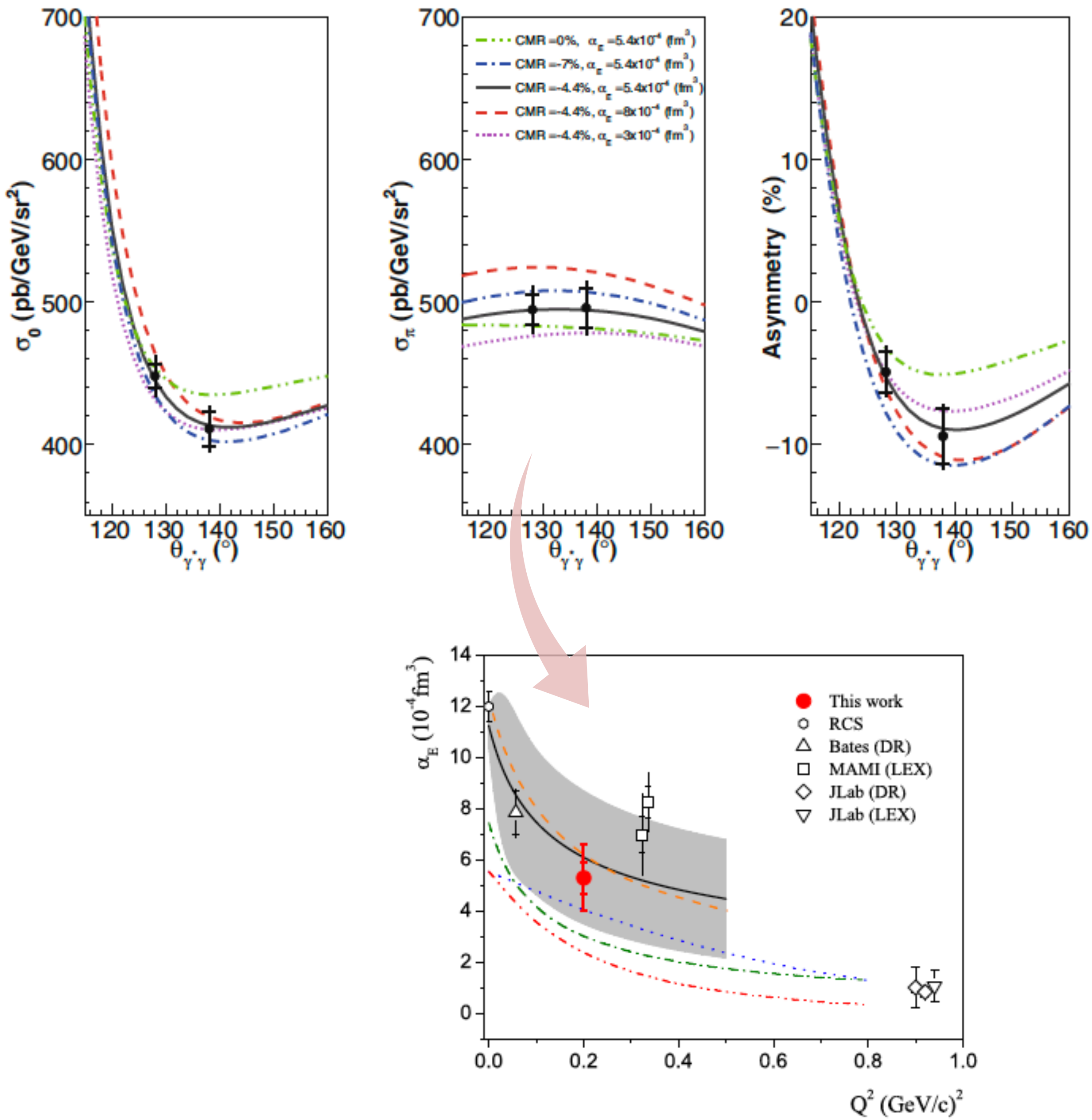

MAMI Results

Phys. Rev. Lett 123, 192302

Phys. Rev. C 103, 025205

Eur. Phys. J. A55, 182

<u>PhD students</u>:

Jure Bericic (Ljubljana Univ.)

Loup Correa (Clermont-Fd Univ.)

Meriem BenAli (Clermont-Fd Univ.)

Adam Blomberg (Temple Univ.)

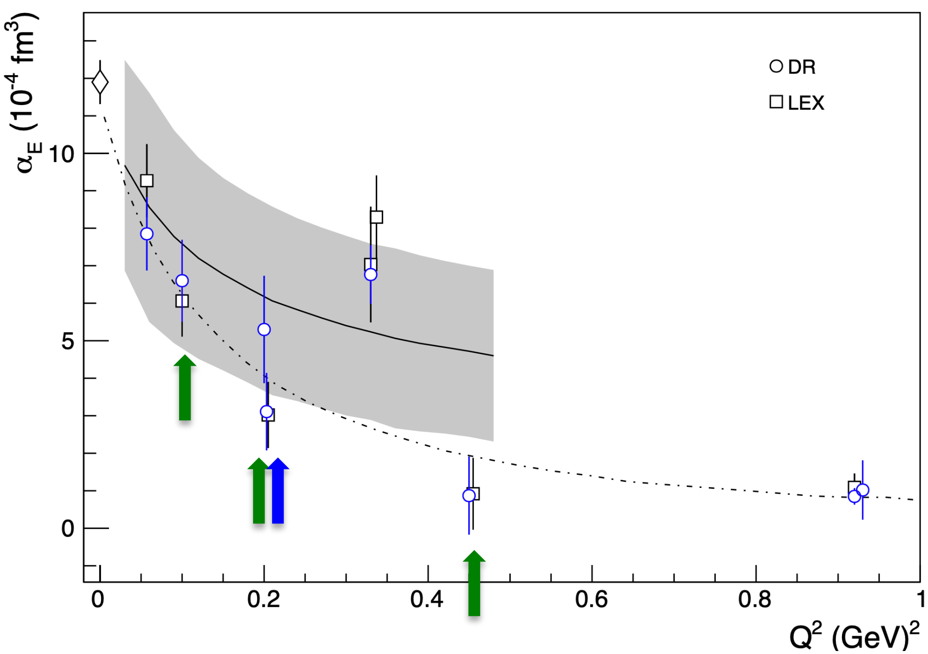

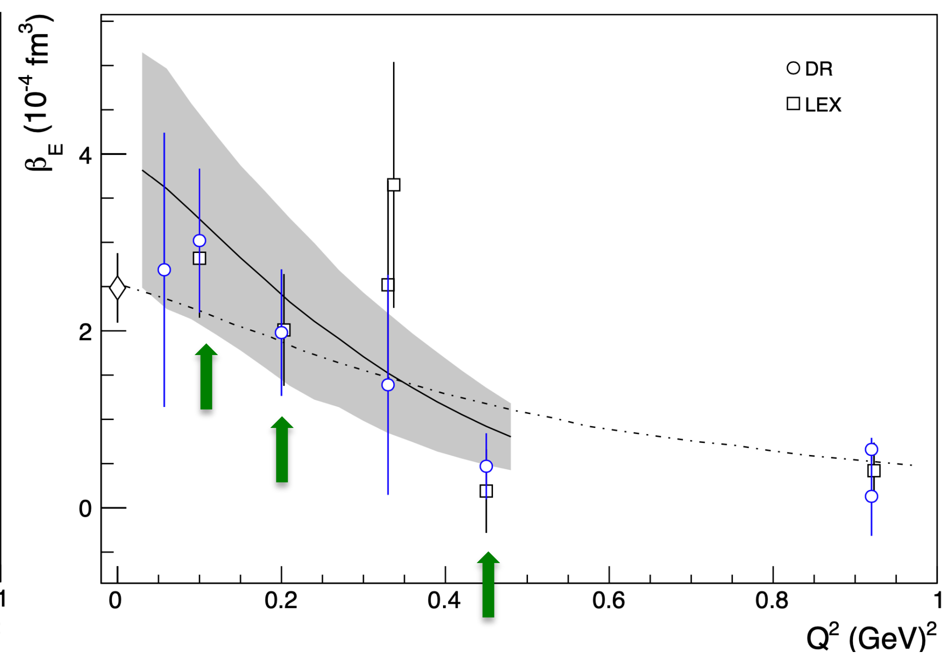

A1/1-09 @ MAMI

A1/3-12 @ MAMI

Revisiting the Q^2=0.33 GeV^2 data

Q^2 = 0.33 $(GeV/c)^2$ measured twice at MAMI - two different experiments

- Phys. Rev. Lett 85, 708 (2000)
- Eur. Phys. J. A37, 1-8 (2008)

Analysis revisited (unpublished):

$\alpha_E(Q^2)$

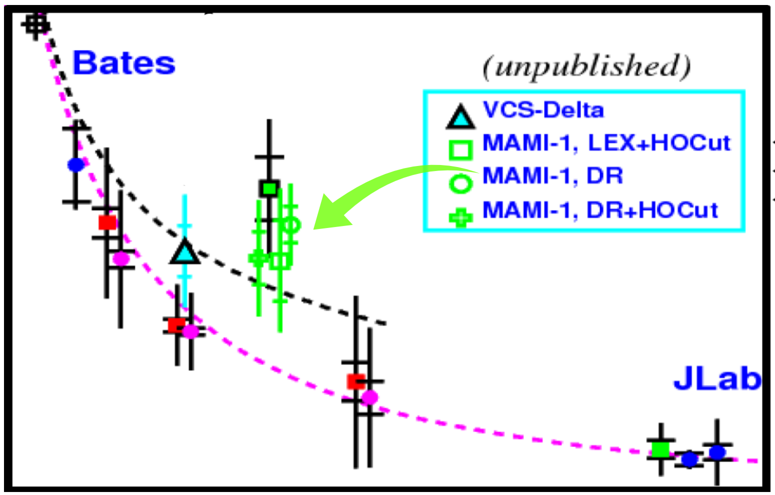

Re-fits at Q^2=0.33 GeV^2 (H.F.)

LEX and DR

Updated HO-cut

The α_E puzzle still holds

$\beta_M(Q^2)$

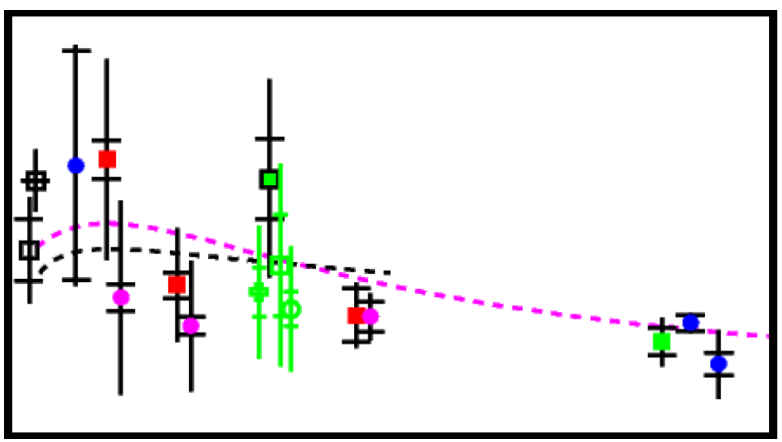

(material from H. Fonvieille)

Experiment E12-15-001: JLab / Hall-C

Conduct measurements with high precision targeting explicitly the kinematical regime of interest

Measure above pion threshold

→ enhanced sensitivity to the GPs

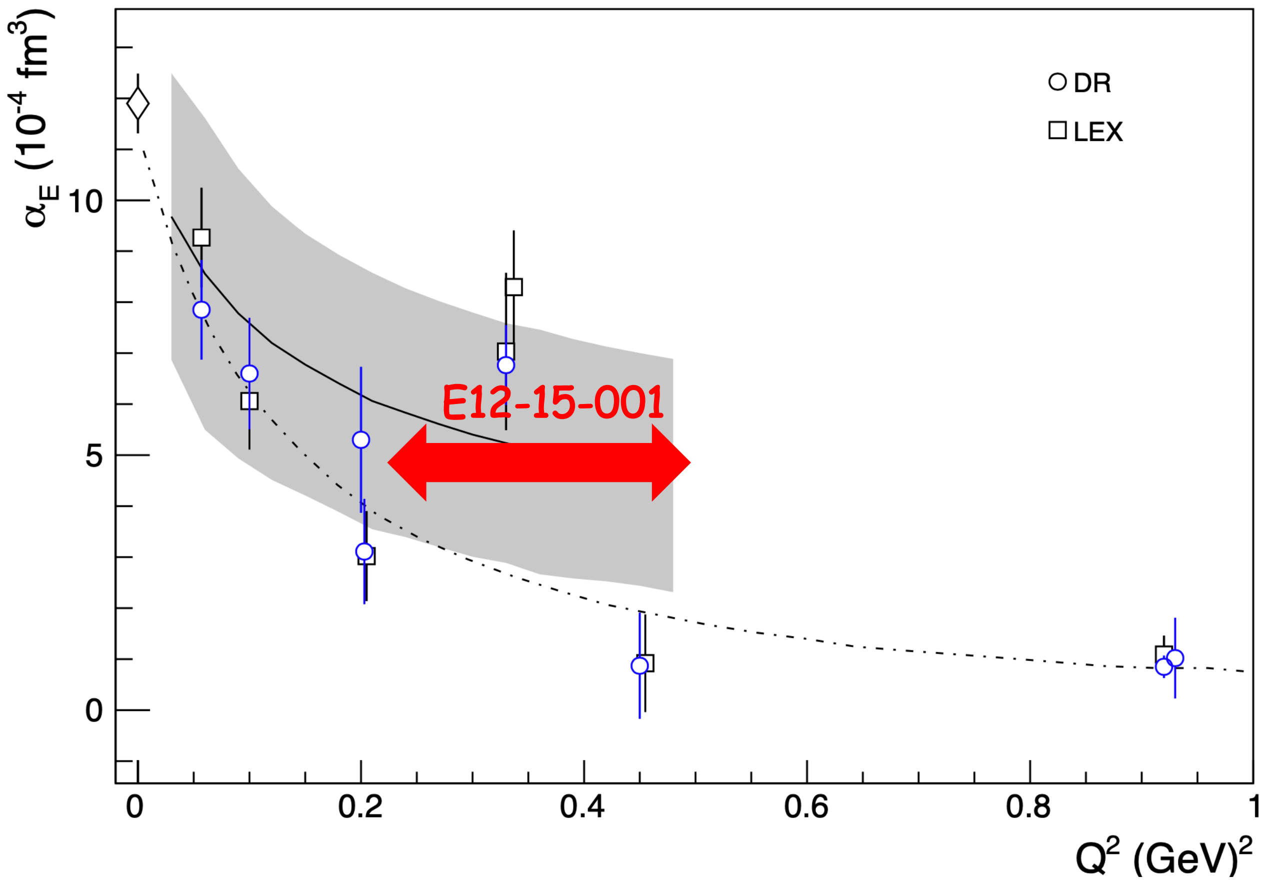

Hall C HMS and SHMS

SHMS:
- 11-GeV Spectrometer
- Partner of existing 6-GeV **HMS**

MAGNETIC OPTICS:
- Point-to Point QQQD for easy calibration and wide acceptance.
- Horizontal bend magnet allows acceptance at forward angles (5.5°)

Detector Package:
- Drift Chambers
- Hodoscopes
- Cerenkovs
- Calorimeter
- All derived from existing HMS/SOS detector designs

- Super High Momentum Spectrometer
  - HB, 3 Quads, Dipole
  - P ➛ 2 - 11 GeV
  - Resolution: $\delta < 0.1\%$
  - Acceptance: δ ➛30%, 4 msr
  - $5.5° < \theta < 40°$
  - Good e/π/K/p PID
- High Momentum Spectrometer
  - 3 Quads, Dipole
  - P ➛ 7.5 GeV
  - Resolution: $\delta < 0.1\%$
  - Acceptance: δ ➛18%, 6.5 msr
  - $10.5° < \theta < 90°$
  - Good e/π/K/p PID

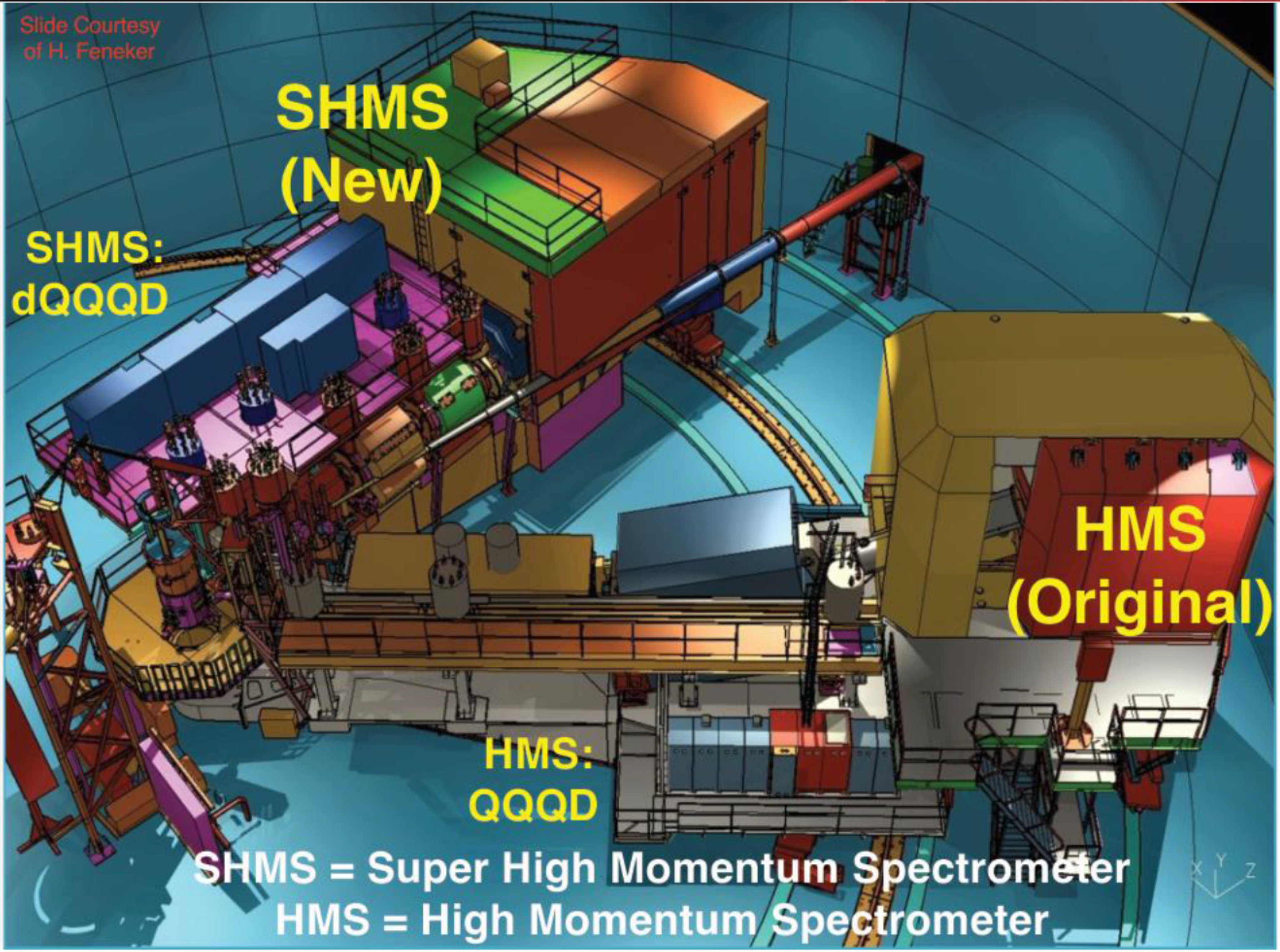

The experiment

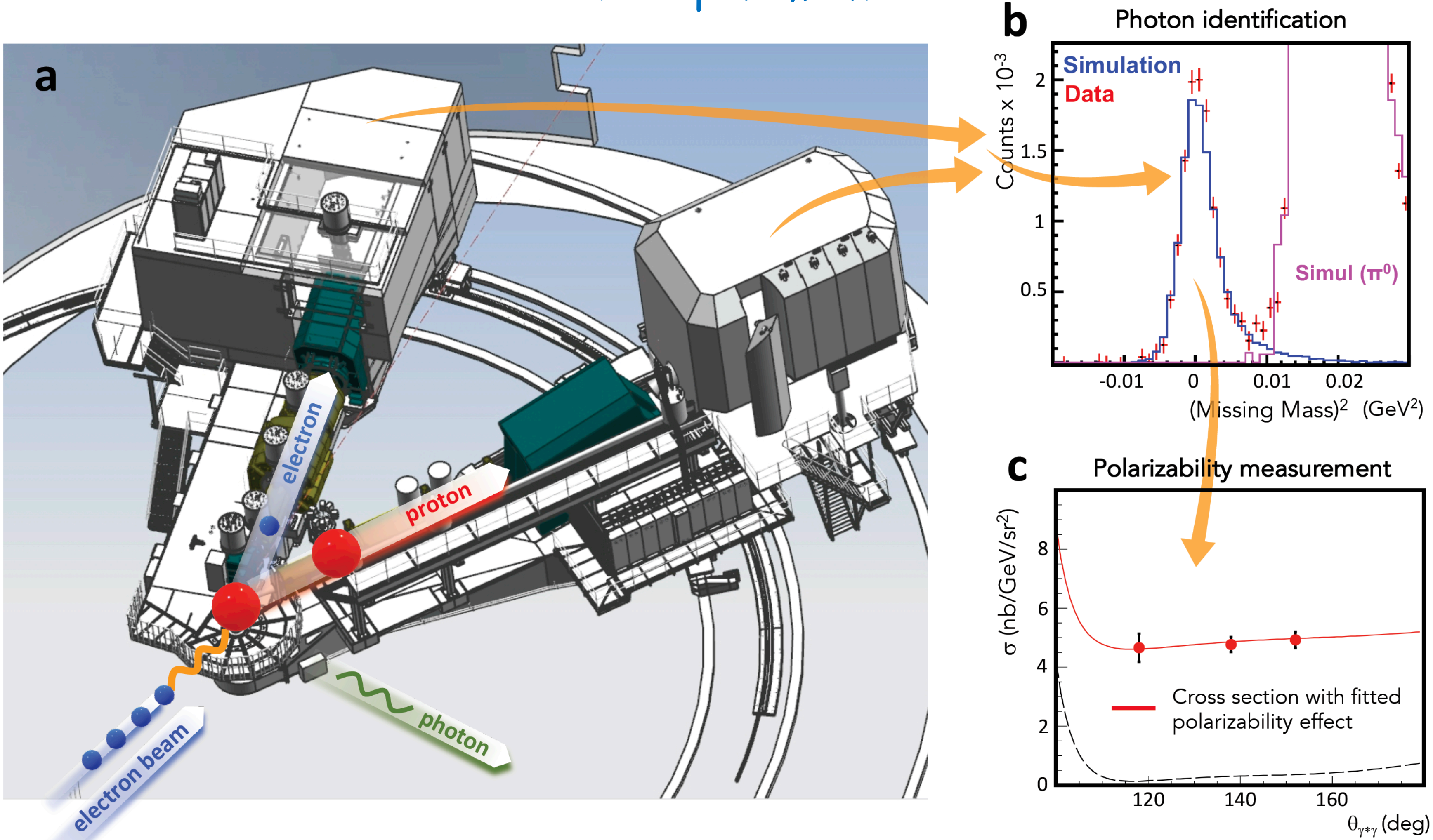

Hall C: SHMS, HMS

4.56 GeV

20 μA

Liquid hydrogen 10 cm

cross sections & azimuthal asymmetries

$$A_{(\phi_{\gamma^*\gamma}=0,\pi)} = \frac{\sigma_{\phi_{\gamma^*\gamma}=0} - \sigma_{\phi_{\gamma^*\gamma}=180}}{\sigma_{\phi_{\gamma^*\gamma}=0} + \sigma_{\phi_{\gamma^*\gamma}=180}}$$

sensitivity to GPs

suppression of systematic asymmetries

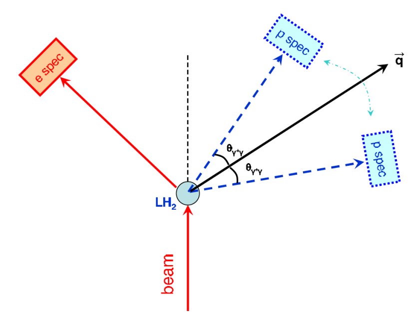

Projected Measurements

$Q^2 = 0.4\ (GeV/c)^2$

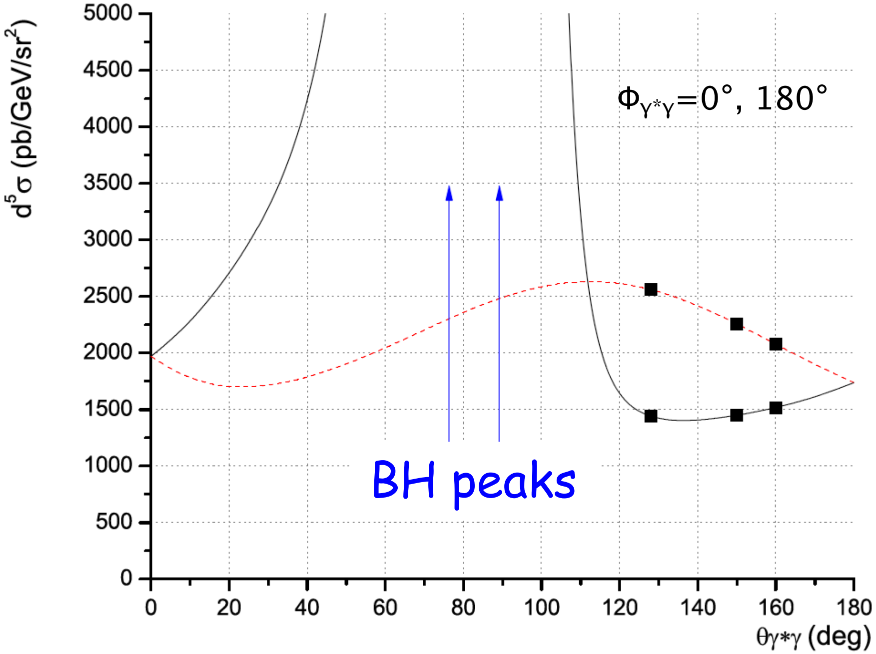

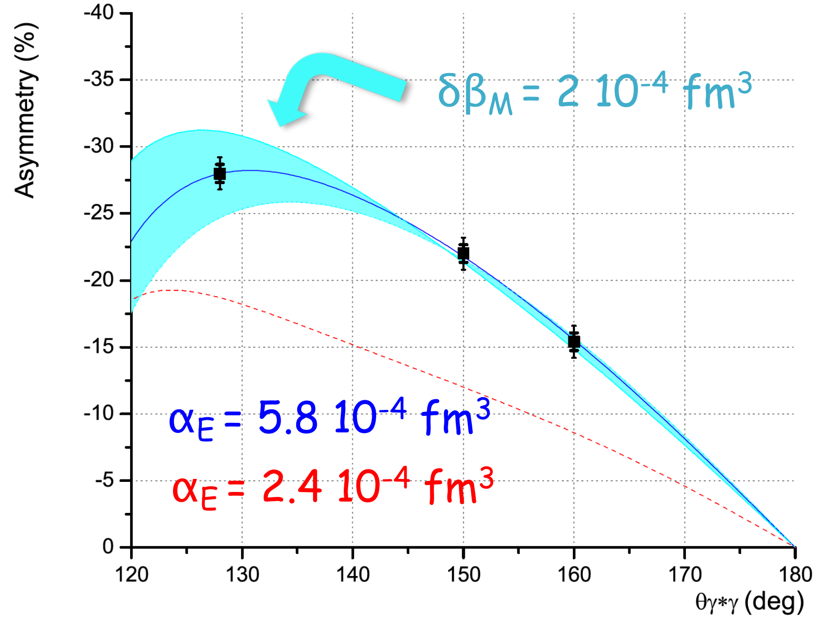

avoid BH region

stay above $\theta_{\gamma^*\gamma} > 120°$

Kinematical Settings

	Kinematical Setting	$\theta_{\gamma^*\gamma}{}^\circ$	$\theta_e{}^\circ$	$P'_e(MeV/c)$	$\theta_p{}^\circ$	$P'_p(MeV/c)$	S/N	beam time (days)
	Kin Ia	155	7.97	3884.4	37.20	893.20	1.1	0.5
	Kin Ib	155	7.97	3884.4	51.26	893.20	2.7	0.5
	Kin IIa	140	7.97	3884.4	33.08	859.90	1	0.45
	Kin IIb	140	7.97	3884.4	55.38	859.90	3.7	0.55
	Kin IIIa	120	7.97	3884.4	27.85	794.68	0.9	0.45
	Kin IIIb	120	7.97	3884.4	60.61	794.68	6.2	0.55
Part I	Kin IVa	165	9.39	3820.5	40.85	1010.40	1.3	0.5
	Kin IVb	165	9.39	3820.5	48.45	1010.40	2.4	0.5
	Kin Va	155	9.39	3820.5	38.34	995.20	1	0.5
	Kin Vb	155	9.39	3820.5	50.96	995.20	3.2	0.5
	Kin VIa	128	9.39	3820.5	31.84	919.43	0.7	0.95
	Kin VIb	128	9.39	3820.5	57.46	919.43	7.8	0.55
	Kin VIIa	165	11.54	3708.6	40.81	1175.25	2.6	1.5
	Kin VIIb	165	11.54	3708.6	47.35	1175.25	5	2
Part II	Kin VIIIa	160	11.54	3708.6	39.73	1167.72	2.2	1.5
	Kin VIIIb	160	11.54	3708.6	48.43	1167.72	6.3	2
	Kin IXa	140	11.54	3708.6	35.52	1117.38	1.2	1.5
	Kin IXb	140	11.54	3708.6	52.64	1117.38	8	2

Part I

$Q^2 = 0.25 - 0.4\ GeV^2$

acquired data in 2019

(results follow in this talk)

Part II

Add more statistics and extend measurements further in Q^2

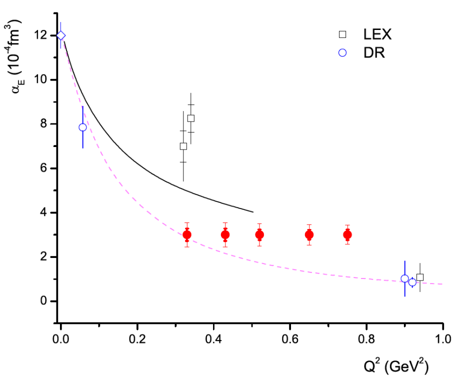

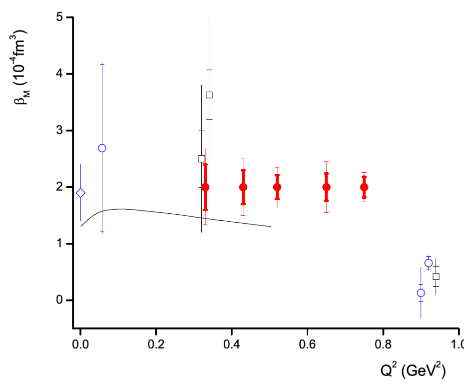

Elastic data

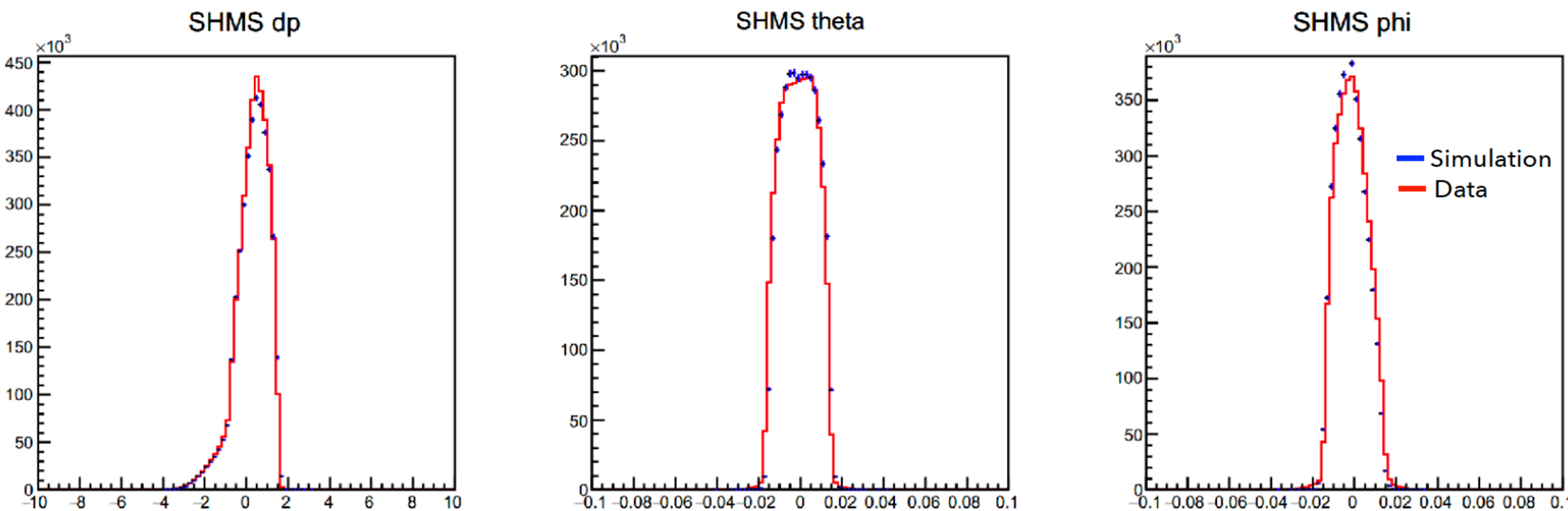

Kinematic	θ_e°	$P_e(GeV/c)$	θ_p°	$P_p(GeV/c)$
Elastic I	10.76	4.193	61.16	0.893
Elastic II	10.41	4.214	61.95	0.863
Elastic III	9.64	4.259	63.76	0.795

p(e,e'p)π⁰

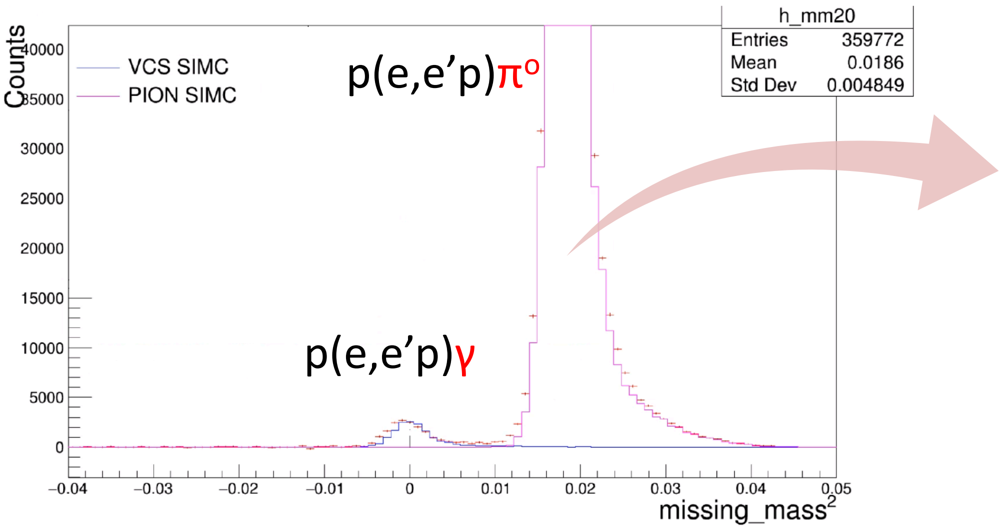

Counts
VCS SIMC
PION SIMC
p(e,e'p)π°
p(e,e'p)γ
h_mm20
Entries 359772
Mean 0.0186
Std Dev 0.004849
missing_mass²

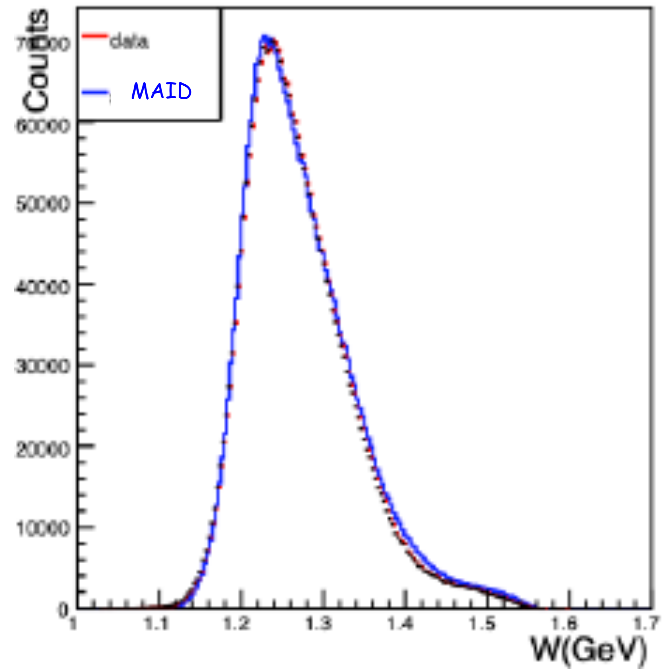

Counts
data
MAID
W(GeV)

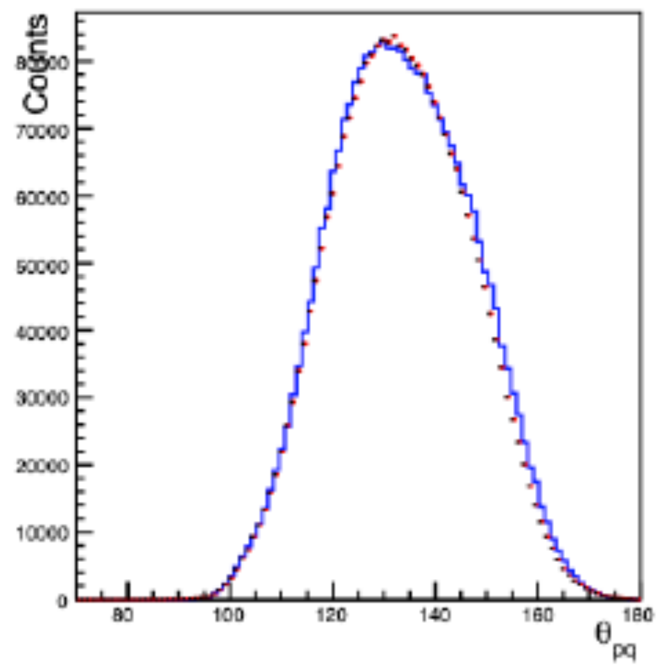

Counts
θ_pq

N→Δ TFFs

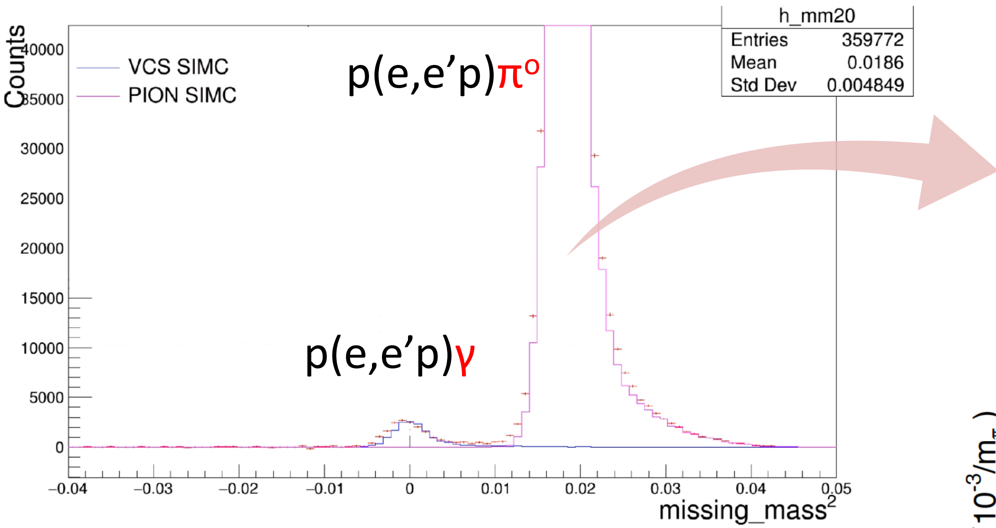

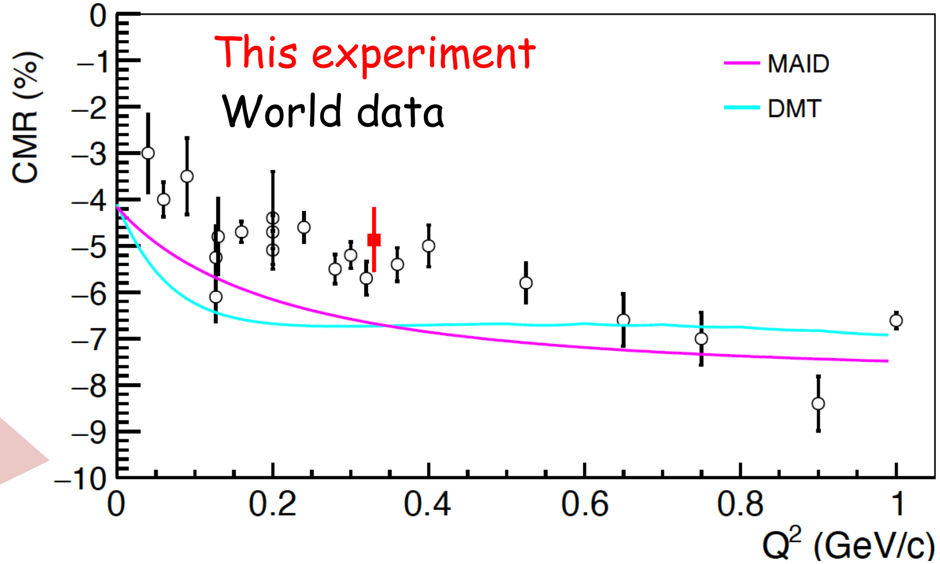

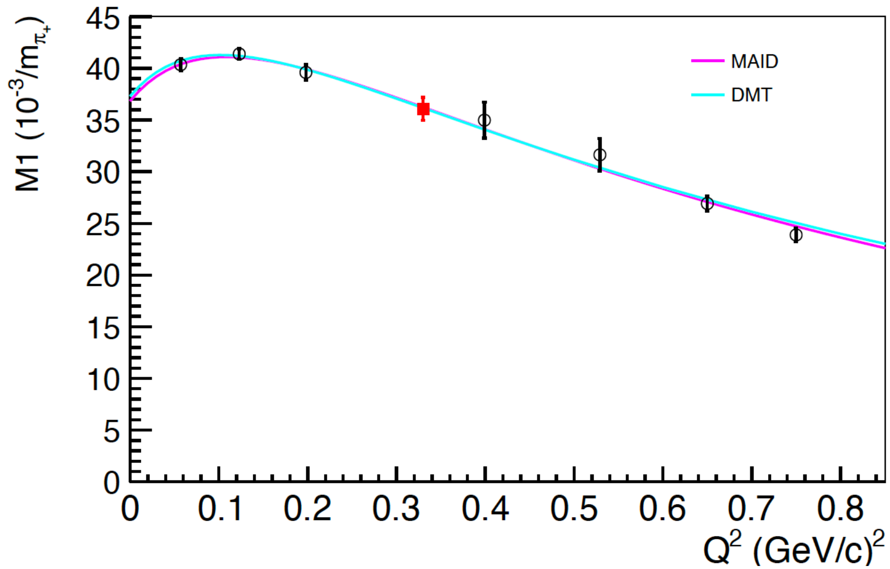

Simultaneous measurement of the N→Δ TFFs

TFFs well known
→ normalization control in real-time

Good understanding of spectrometer acceptance

New results: VCS cross sections

Q^2=0.27 GeV^2

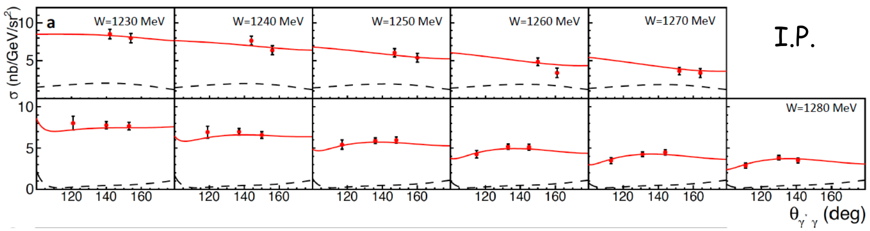

I.P.

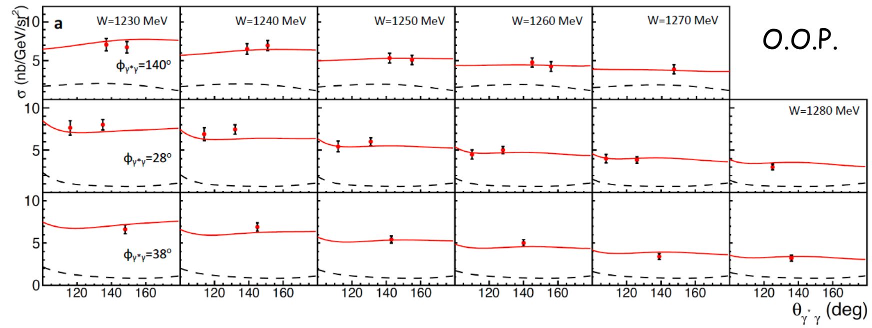

O.O.P.

Q^2=0.33 GeV^2

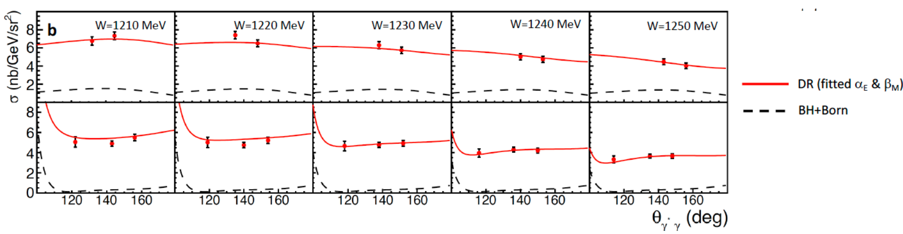

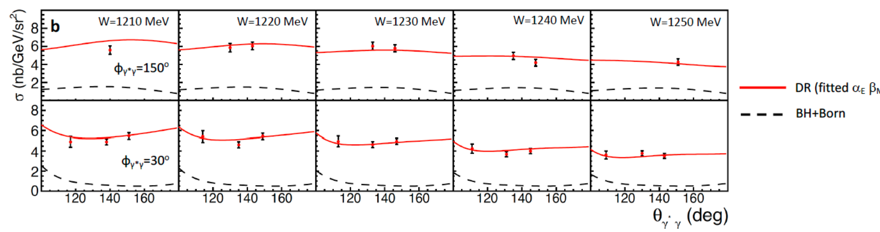

Q^2=0.40 GeV^2

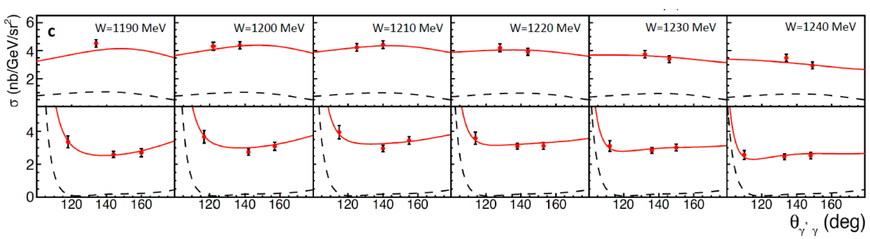

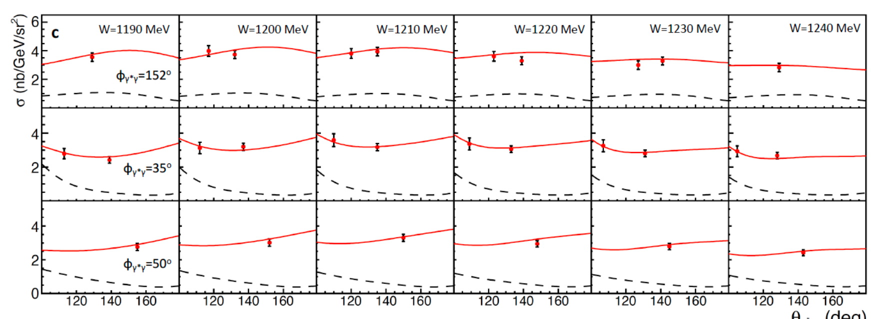

New results: GPs

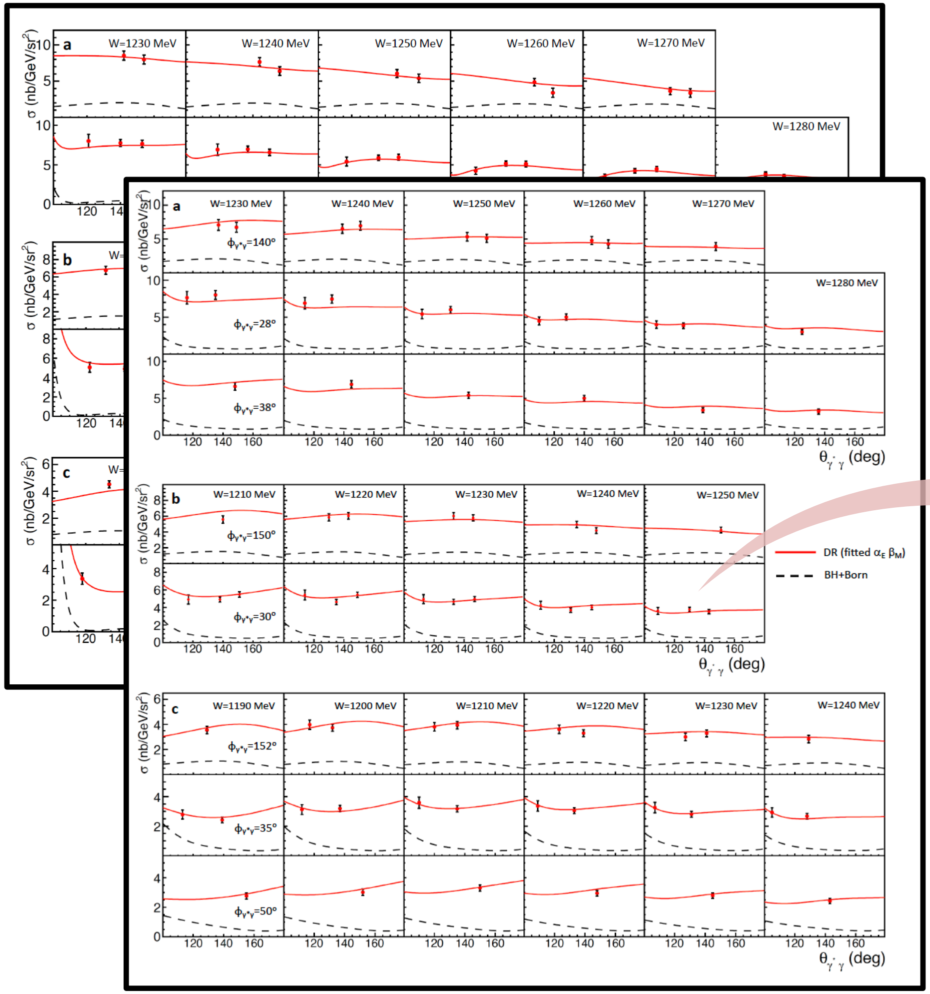

DR fit

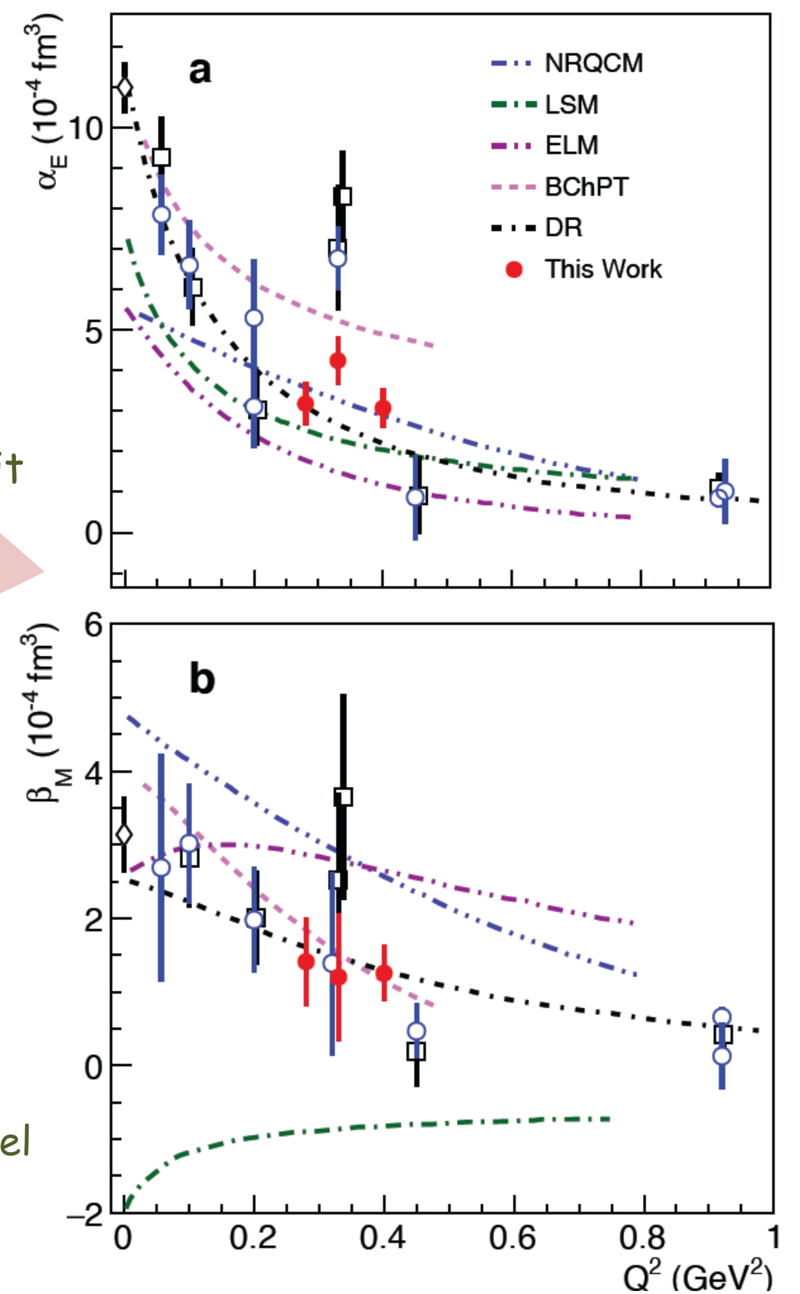

Experimental cross sections are compared to the DR model predictions for all possible values for the GPs

→ $\alpha_E(Q^2)$ and $\beta_M(Q^2)$ are fitted by a χ^2 minimization

MAMI-I re-analysis (unpublished)

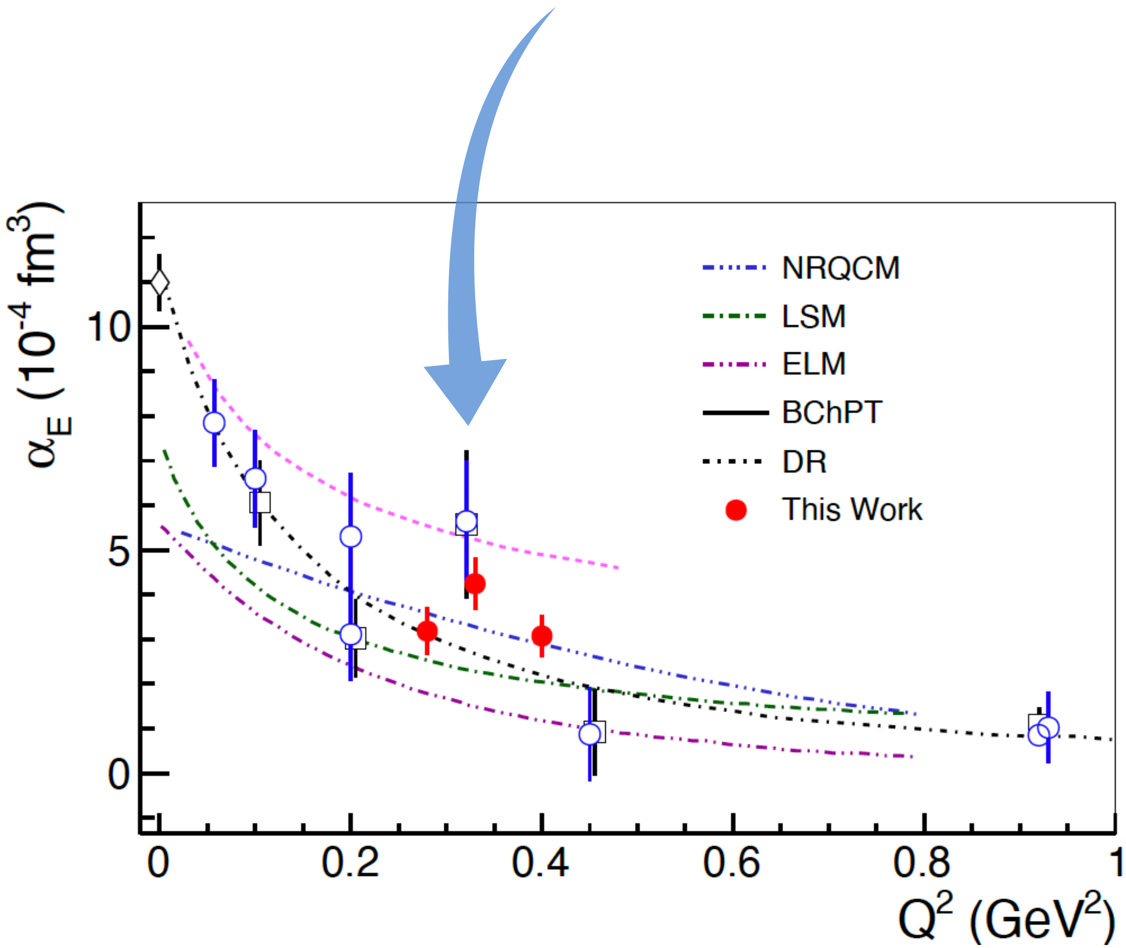

Ruonan Li (Temple Univ.)
Hamza Atac (Temple Univ.)
Mark Jones (JLab.)
Michael Paolone (NMSU)

Paper under review

Q^2 dependence of the electric GP

Traditional fits using

predefined functional forms

Data-driven techniques

no direct underlying functional form is assumed

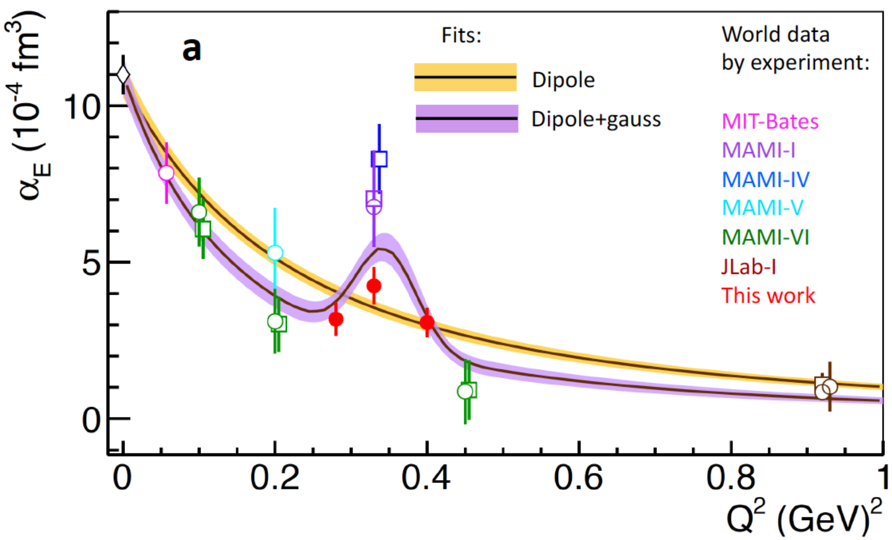

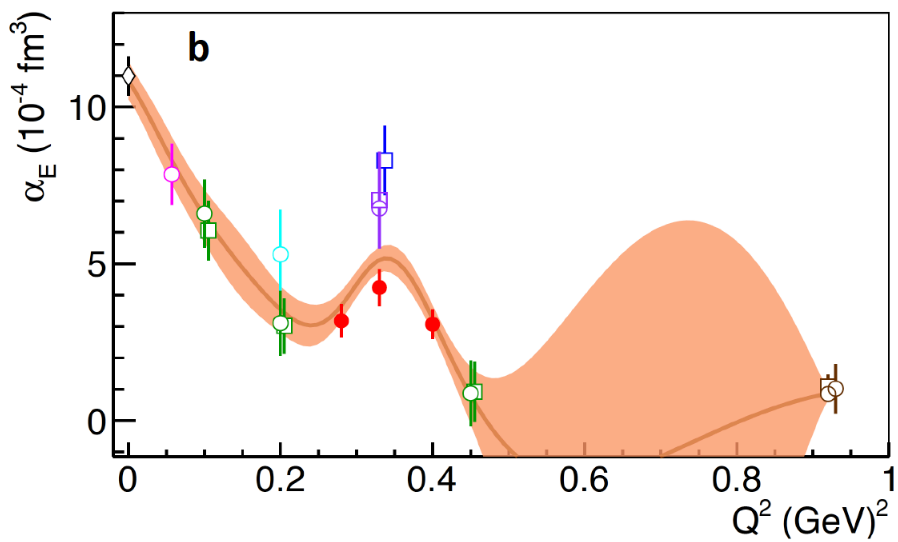

Dipole (?) (χ^2_ν=3.7)

Systematically overestimates MAMI-VI

Systematically underestimates MAMI-I & IV

Cuts grossly through the new measurements

Rasmussen, C. E., and Williams, C. K. I. *Gaussian Processes for Machine Learning* the MIT Press, Cambridge Massachusetts, 2006, ISBN 026218253X, ©2006 Massachusetts Institute of Technology.

Spatial dependence of induced polarizations on an external EM field

Nucleon form factor data ➔ light-front quark charge densities

Formalism extended to the deformation of these quark densities when applying an external e.m. field:

GPs ➔ spatial deformation of charge & magnetization densities under an applied e.m. field

Induced polarization in a proton when submitted to an e.m. field

Phys. Rev. Lett. 104, 112001 (2010)

M. Gorchtein, C. Lorce, B. Pasquini, M. Vanderhaeghen

GP I   GP II

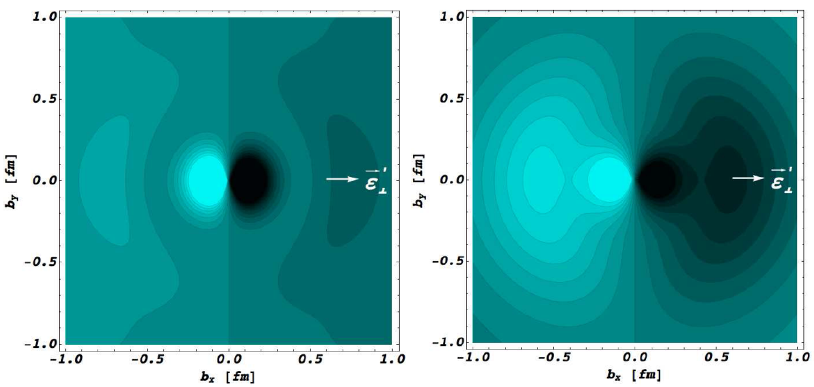

Light (**dark**) regions ➔ **largest** (**smaller**) values

(photon polarization along x-axis, as indicated)

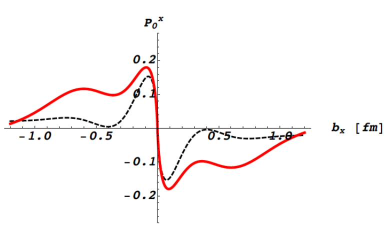

Induced polarization along b_y=0

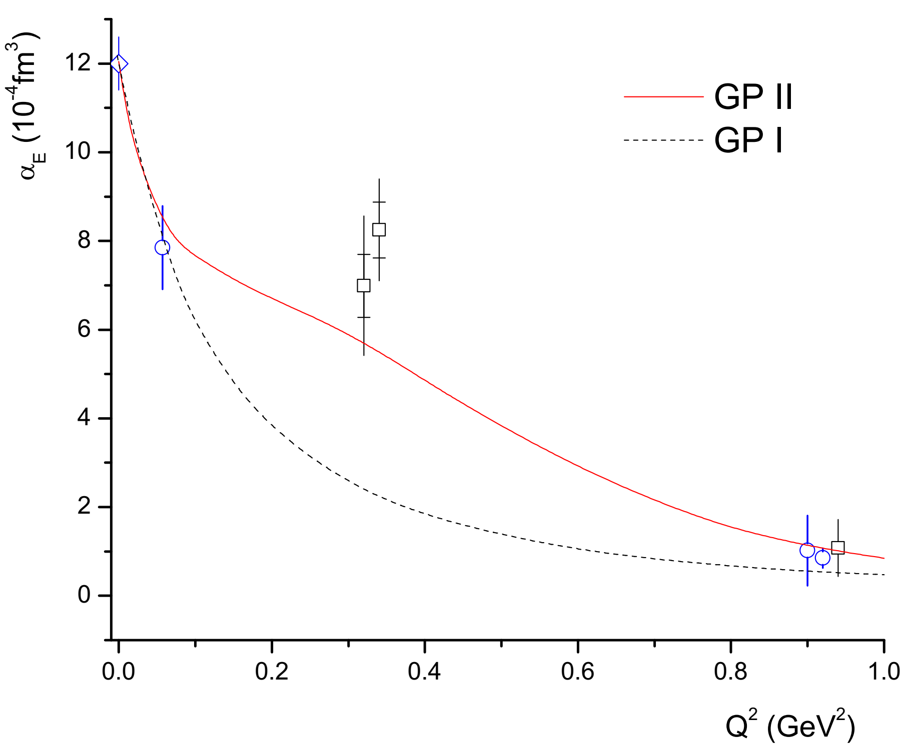

Spatial dependence of induced polarizations on an external EM field

Nucleon form factor data ➔ light-front quark charge densities

Formalism extended to the deformation of these quark densities when applying an external e.m. field:

GPs ➔ spatial deformation of charge & magnetization densities under an applied e.m. field

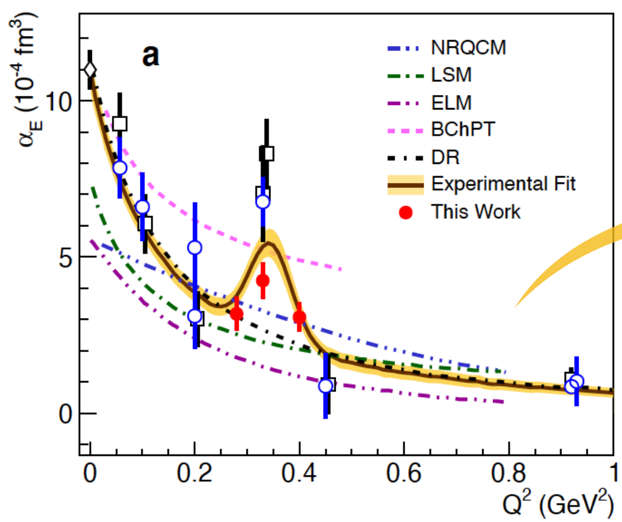

Induced polarization in a proton when submitted to an e.m. field

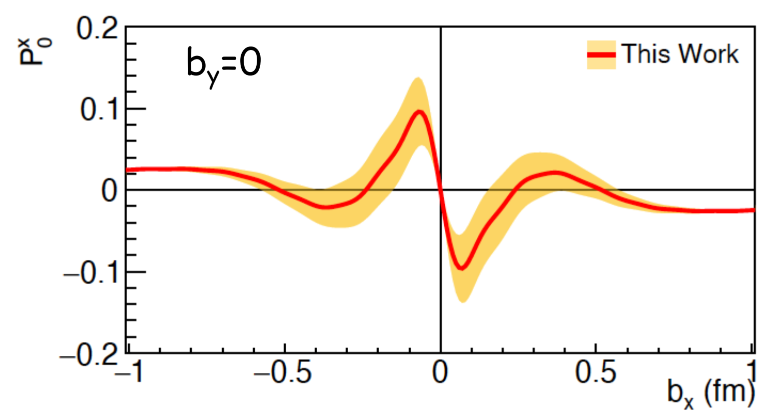

x-y defines the transverse plane with the z-axis being the direction of the fast-moving proton

Polarizability radii

$$\langle r^2_{\alpha_E} \rangle = \frac{-6}{\alpha_E(0)} \cdot \frac{d}{dQ^2}\alpha_E(Q^2)\Big|_{Q^2=0}$$

$$\langle r^2_{\beta_M} \rangle = \frac{-6}{\beta_M(0)} \cdot \frac{d}{dQ^2}\beta_M(Q^2)\Big|_{Q^2=0}$$

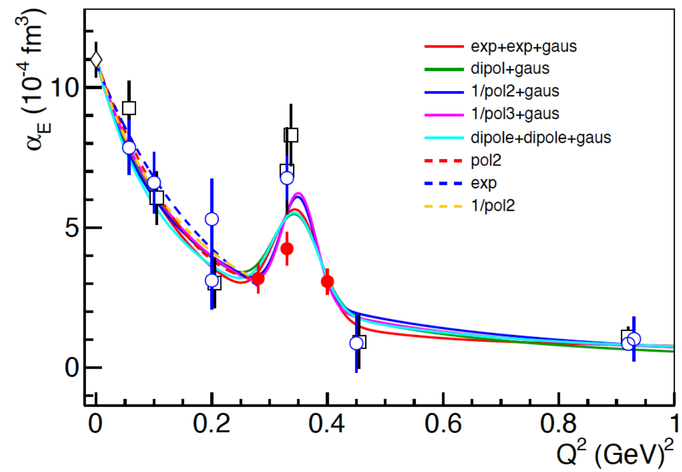

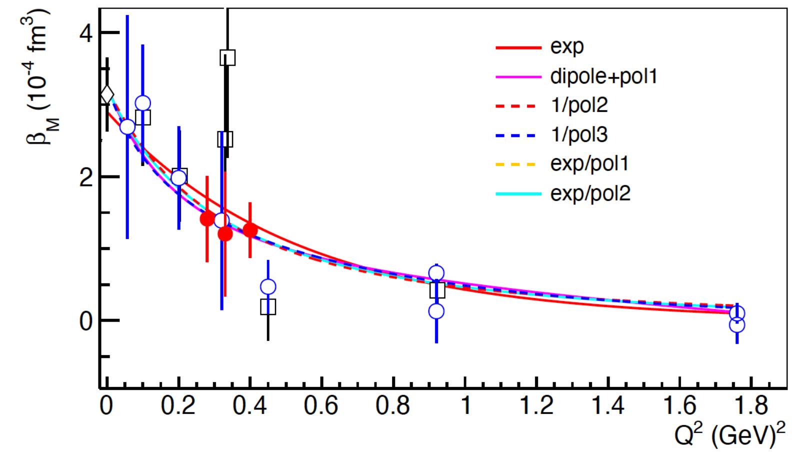

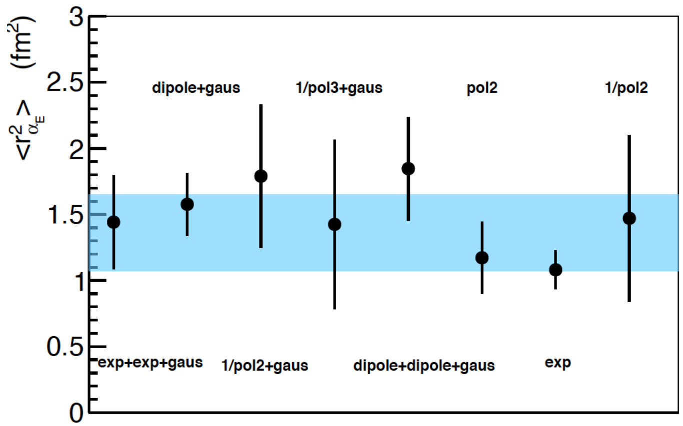

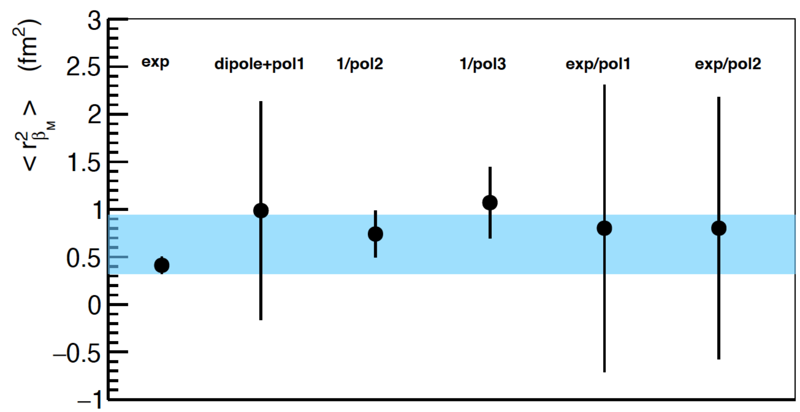

$$\langle r^2_{\alpha_E} \rangle = 1.36 \pm 0.29 \text{ fm}^2$$

$$\langle r^2_{\beta_M} \rangle = 0.63 \pm 0.31 \text{ fm}^2$$

Polarizability radii

$$\langle r^2_{\alpha_E} \rangle = \frac{-6}{\alpha_E(0)} \cdot \frac{d}{dQ^2}\alpha_E(Q^2)\Big|_{Q^2=0}$$

$$\langle r^2_{\beta_M} \rangle = \frac{-6}{\beta_M(0)} \cdot \frac{d}{dQ^2}\beta_M(Q^2)\Big|_{Q^2=0}$$

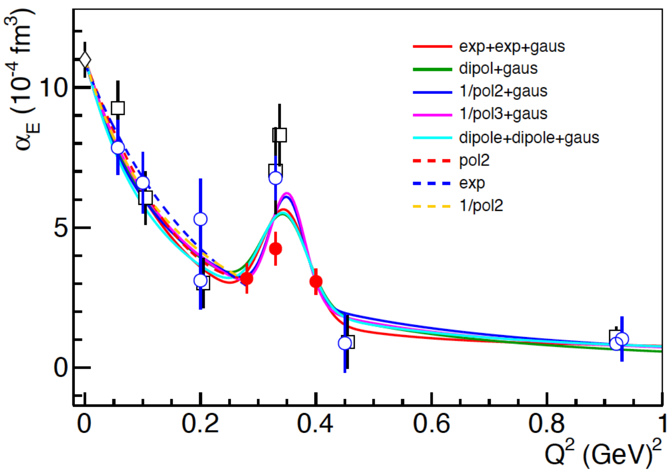

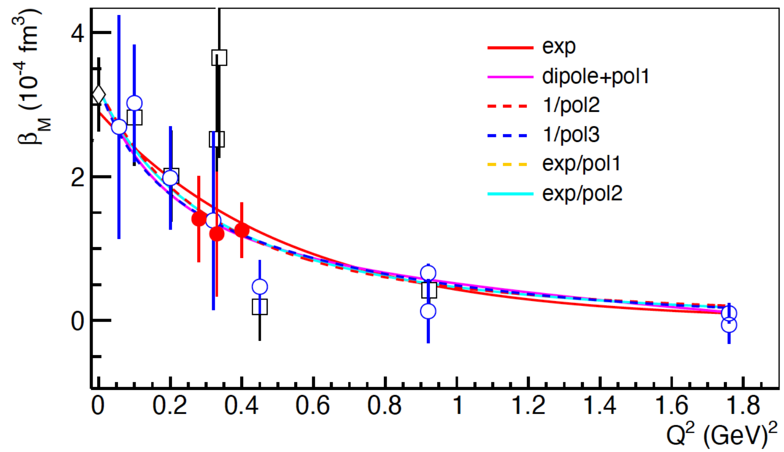

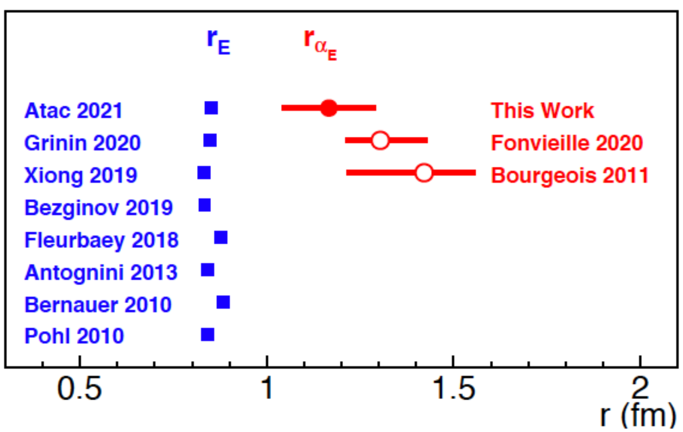

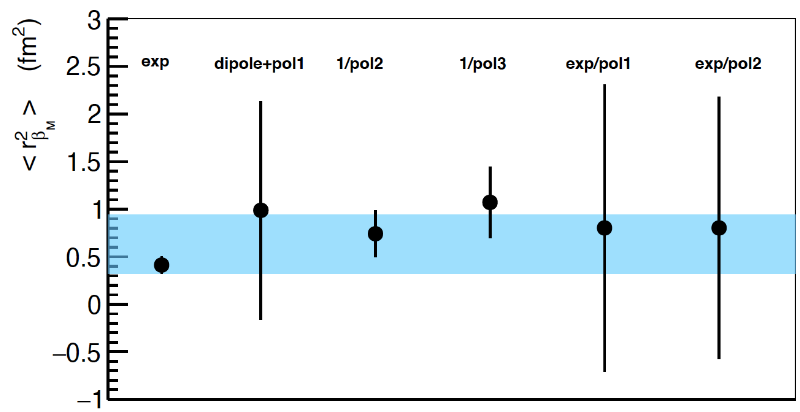

$$\langle r^2_{\alpha_E} \rangle = 1.36 \pm 0.29 \text{ fm}^2$$

$$\langle r^2_{\beta_M} \rangle = 0.63 \pm 0.31 \text{ fm}^2$$

Moving forward

VCS-II at JLab (Hall-C): new JLab proposal for JLab PAC51 (summer 2023):

targeted measurements in the area of interest, higher & lower in Q^2

Eur. Phys. J. A 57 (2021) 11, 316

Virtual Compton scattering at low energies with a positron beam

Barbara Pasquini[a,1,2], Marc Vanderhaeghen[b,3]

[1]Dipartimento di Fisica, Università degli Studi di Pavia, 27100 Pavia, Italy
[2]Istituto Nazionale di Fisica Nucleare, Sezione di Pavia, 27100 Pavia, Italy
[3]Institut für Kernphysik and PRISMA+ Cluster of Excellence, Johannes Gutenberg Universität, D-55099 Mainz, Germany

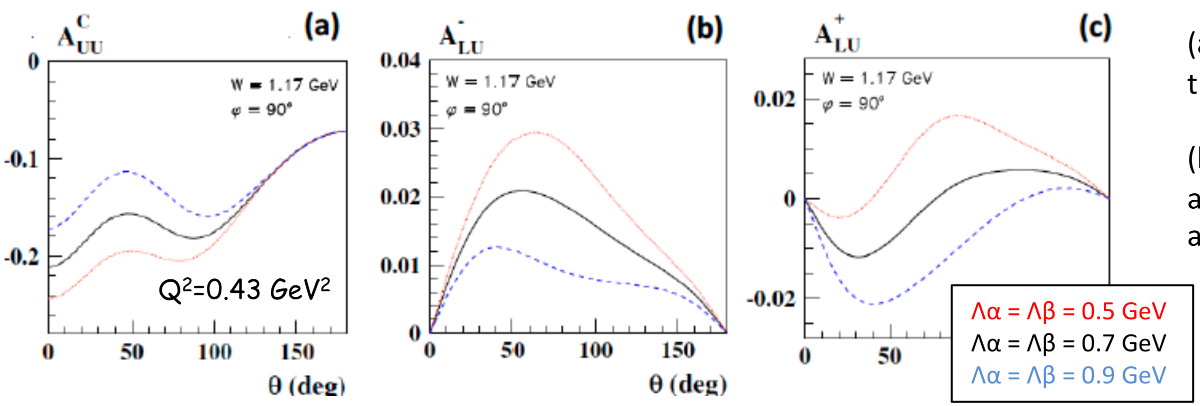

(a): The beam-charge asymmetry as a function of the photon scattering angle at Q2 = 0.43 GeV 2.

(b) & (c): The electron and positron beam-spin asymmetry as a function of the photon scattering angle for out-of-plane kinematics.

Challenges for the theory - in particular for $\alpha_E(Q^2)$

Summary

New high precision measurements of fundamental system properties (GPs)

Insight to spatial deformation of the nucleon densities under an applied e.m. field, interplay of paramagnetism-diamagnetism in the proton, polarizability radii

A non-trivial behavior in $\alpha_E(Q^2)$ is confirmed albeit with a smaller magnitude than originally suggested

Challenge for the theory with respect to $\alpha_E(Q^2)$

High precision benchmark data for theory - strong constraints to the theoretical predictions

Future experimental measurements can explore in more detail –
pinning down precisely the shape of the structure is important input for the theory

Future LQCD calculations will be of great interest

Thank you!